Lateral Line Ablation by Ototoxic Compounds Results in Distinct Rheotaxis Profiles in Larval Zebrafish

Kyle C Newton[1,5]*, Dovi Kacev[2], Simon R O Nilsson[3], Allison L Saettele[1], Sam A Golden[3], and Lavinia Sheets[1,4]*

[1] Department of Otolaryngology, Washington University School of Medicine, St. Louis, MO, USA

[2] Scripps Institution of Oceanography, University of California San Diego, La Jolla, CA, USA

[3] Department of Biological Structure, University of Washington, Seattle, WA, USA

[4] Department of Developmental Biology, Washington University School of Medicine, St. Louis, MO, USA

*** Correspondence:**

Kyle C Newton (kylecnewton@gmail.com; kyle.newton@oregonstate.edu)

[5] K C Newton's current affiliation: Department of Fisheries, Wildlife and Conservation Sciences, Coastal Oregon Marine Experiment Station, Oregon State University, Hatfield Marine Science Center, Newport, OR, USA

Lavinia Sheets (sheetsl@wustl.edu)

Keywords: zebrafish, lateral line, neuromast, sensory hair cell, rheotaxis, pose estimation, animal tracking, behavior classification, behavioral profile, machine learning, machine vision

ABSTRACT

The zebrafish lateral line is an established model for hair cell organ damage, yet few studies link mechanistic disruptions to changes in biologically relevant behavior. We used larval zebrafish to determine how damage via ototoxic compounds impact rheotaxis. Larvae were treated with $CuSO_4$ or neomycin to disrupt lateral line function then exposed to water flow stimuli. Their swimming behavior was recorded on video then DeepLabCut and SimBA software were used to track movements and classify rheotaxis behavior, respectively. Lateral line-disrupted fish performed rheotaxis, but they swam greater distances, for shorter durations, and with greater angular variance than controls. Furthermore, spectral decomposition analyses confirmed that lesioned fish exhibited ototoxic compound-specific behavioral profiles with distinct changes in the magnitude, frequency, and cross-correlation between fluctuations in linear and angular movements. Our observations demonstrate that lateral line input is needed for fish to hold their station in flow efficiently and reveals that commonly used lesion methods have unique effects on rheotaxis behavior.

INTRODUCTION

The lateral line is a sensory system used by fishes and amphibians to detect water flow. The functional units of the lateral line are neuromasts; bundles of sensory hair cells located externally along the head and body that mechanotransduce low frequency (≤ 200 Hz) water flow stimuli into electrochemical signals for interpretation by the central nervous system (reviewed in [1]). The lateral line is known to partially mediate rheotaxis, a multimodal behavior ([2]) that integrates input from visual ([3], [4], [5]), vestibular ([6], [7]), tactile ([3], [8], [9], [10]), and lateral line systems ([9], [10], [8]) to facilitate fish orientation and movement of fish with respect to water flow ([9], [10]).

Although the contribution from the lateral line is well established, there is conflicting evidence on whether it is essential for rheotaxis in fish ([2], [5], [9], [10], [11], [12]). Inconsistent methodologies used on distinct fish species that differentially rely on the lateral line to mediate

49 swimming behaviors obfuscate the relationship between the lateral line and rheotaxis. In
50 addition, a recent review hypothesized that differences in the spatial characteristics and velocity
51 of the flow stimuli used to assay rheotaxis likely resulted in the disparate results reported in
52 these studies (see Table 1 in [13]).

53 Zebrafish hair cells demonstrate unique regenerative features that make them an
54 important model for hearing loss research ([14], [15], [16], [17], [18], [19]). Many studies have focused on
55 mechanistic disruption of hair cell activity, but few have explored the association between
56 disruption and hair cell mediated behavior. Previous researchers have developed several
57 different assays to study rheotaxis in larval fishes (e.g., [5], [20], [21], [22]). However, we sought to
58 develop a behavioral assay and analytical methodology that is sensitive, spatiotemporally
59 scalable, and robust enough to be used on a variety of species, ontogenetic stages, sensory
60 modalities, and behavioral responses that are pertinent to biomedical and ecological research.

61 We therefore investigated how the lateral line contributes to rheotaxis in larval zebrafish
62 and developed a standardized assay that could identify subtle differences in rheotaxis behavior
63 ([12]). We compared the rheotaxis response of fish with an intact lateral line to those with lateral
64 line hair cells ablated by two commonly used compounds: copper sulfate ($CuSO_4$; [17], [23], [24], [25])
65 and neomycin ([5], [15], [26]). We hypothesized that different ototoxic compounds might produce
66 distinct changes in rheotaxis behavior because they injure lateral lines via different cellular
67 mechanisms ([27]), and that these behavioral changes could be empirically quantified using
68 machine vision and learning technology.

69

70 **RESULTS & DISCUSSION**

71 To determine the contribution of the lateral line to rheotaxis in fishes, we used $CuSO_4$
72 and neomycin to ablate the lateral line neuromasts of larval zebrafish (6-7 days post-fertilization
73 (dpf)), then video recorded the swimming behavior of individual larvae in a microflume under no-

flow and flow stimulus conditions (Fig. 1). Our procedures eliminated visual and linear acceleration cues (see methods) and young larval zebrafish cannot detect horizontal angular

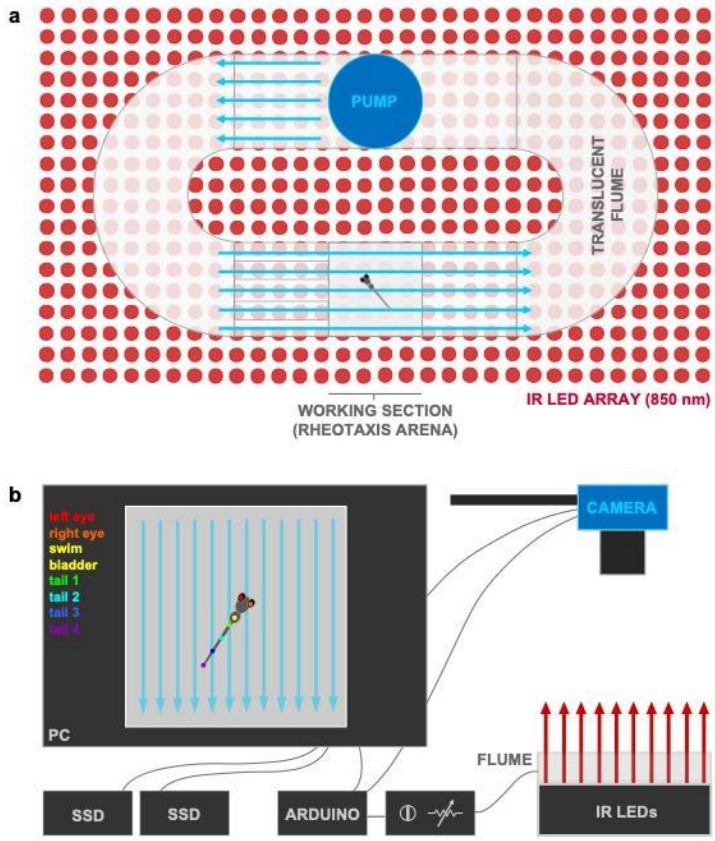

Figure 1. Experimental microflume used to conduct rheotaxis assays under IR illumination. a) The microflume (220 x 100 x 40 mm) with a removeable working section (30 x 30 x 10 mm) was 3D printed from translucent resin and placed on top of an infrared (850 nm) LED array. b) Schematic of experimental set-up. The IR light passed through the flume and the overhead camera recorded rheotaxis trials at either 200 or 60 fps onto SD cards. The timing and duration for the camera and flume pump onset and offset of was controlled by an Arduino and pump voltage (i.e., water flow velocity = 9.74 mm s^{-1}) was controlled by a rheostat. Each trial was monitored via the live camera feed displayed on the PC and all videos were copied in duplicate onto a 12TB RAID array. Dots on fish larva indicate seven body positions tracked by DeepLabCut.

velocity cues (i.e., yaw; [31], [32]); however, it was not possible to selectively block tactile cues in a non-invasive manner. To confirm ablation of lateral line neuromasts, a subset of all fish that had undergone behavioral testing were fixed, then proceed for immunolabeling of hair cells and

88 innervating afferent neurons (Fig. 2). We observed near total hair cell loss in both anterior and
89 posterior lateral line neuromasts with $CuSO_4$ treatment (Fig. 2 a, b, d, e, g) and a significant
90 impact on the morphology and reduction in hair cell number per neuromast following neomycin
91 treatment (Fig. 2 a, c, d, f, g). These results support that the ototoxic compound-treated fish
92 used in our behavior assay had a total absence or severe impairment of lateral line function.
93

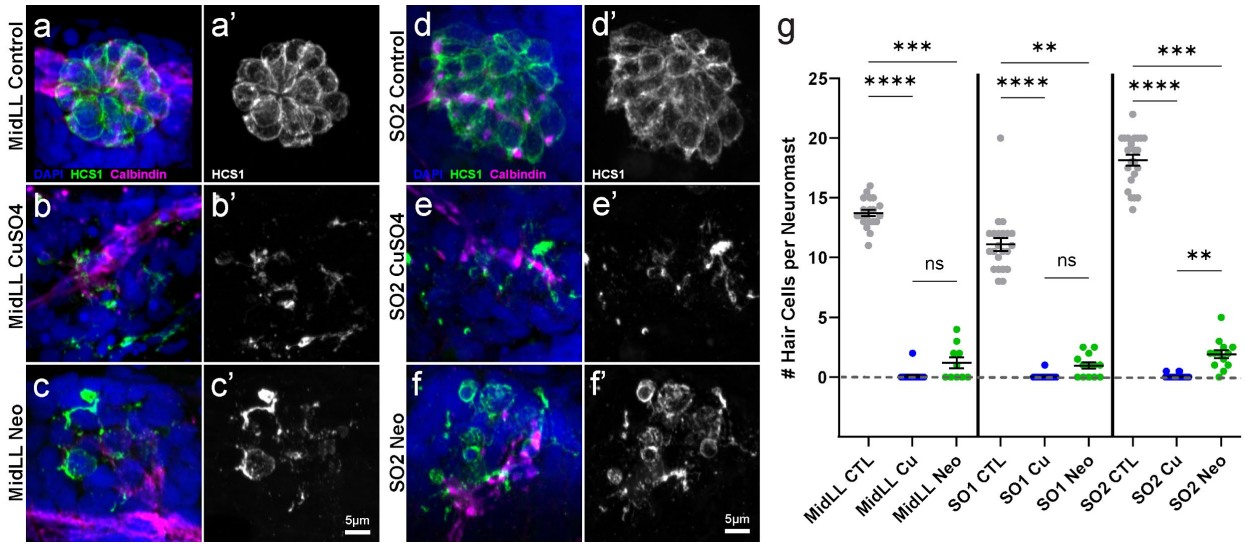

94

95 **Figure 2. Confirmation of neuromast hair cell loss following $CuSO_4$ or neomycin treatment.** a-f) Representative confocal max
96 intensity projection images of the: a-c) mid posterior lateral line (MidLL) fourth neuromast (L4); and d-f) second anterior supraorbital
97 (SO2) neuromast from the fish cohorts used for behavior experiments. Hair cells were labeled with an antibody against Otoferlin
98 (HCS1; green a-f, gray a'-f'). Afferent neurons were labeled with an antibody against Calbindin (magenta), and cell nuclei were
99 labeled with DAPI (blue). g) Quantification of the grand mean (± SEM) number of hair cells per neuromast in intact (CTL), CuSO4-
100 and neomycin-treated fish. Each dot represents the mean number of hair cells from the MidLL (L3, L4, and L5) or SO (left and right)
101 neuromasts from an individual fish. Data were collected from fish used in three experimental behavior trials; 4-6 fish per condition
102 per trial. Significance values: ** < 0.01, ***< 0.001, **** < 0.0001
103

104 We used machine vision and learning software for 3D pose estimation, movement
105 tracking, and annotation of videos for positive rheotaxis events (as defined in methods) when
106 fish oriented toward (0° ± 45°) and actively swam into the oncoming flow (e.g., Supplementary
107 Fig. 1). We standardized our analyses by comparing rheotaxis data acquired during flow to the

swimming behavior of fish when they were randomly oriented at 0° ± 45° under no flow (see data analysis). Under no flow conditions, we determined that each treatment group of fish was randomly distributed (Fig. 3; Supplementary Table 1) and had no natural proclivity to orient their bodies to 0° ± 45° (Supplementary Table S2).

Lateral Line Ablation Alters but Does Not Eliminate Rheotaxis Behavior

We predicted that fish treated with the minimum dosage of $CuSO_4$ or neomycin necessary to ablate lateral line hair cells would not perform rheotaxis as well as control fish with an intact lateral line. Surprisingly, fish with lesioned lateral line organs could still orient into oncoming flow like control fish (Fig. 3; Supplementary Tables 1-2), indicating that the effects of ablation were subtle, and the lateral line was not essential for rheotaxis behavior.

By analyzing the kinematic components of rheotaxis movement, stark behavioral changes were observed among lesioned fish. Comparisons between lateral line-ablated and control groups showed significant differences in the mean body angle or angular variance (Fig. 3, Supplementary Table 3), mean duration of rheotaxis events, mean number of rheotaxis events, total distance traveled, and latency to the onset of rheotaxis (Fig. 4, Supplementary Tables 4-7). These observations demonstrate that rheotaxis occurs but is altered in lateral line-ablated groups, which contrasts with previous reports on larval zebrafish ([5], [22], [28]) and supports the idea that the lateral line is not required for rheotaxis in fishes ([2], [11], [12], [29], [30]).

We posit that our focus on acute rheotaxis behavior (~20 s) and the fine scale spatiotemporal sampling of machine vision technology allowed us to detect subtle changes in behavior that were overlooked in previous rheotaxis studies ([2], [5], [12], [29], [30]). Our methods eliminated turbulent water flow, optic flow ([3]), and certain vestibular cues (yaw: [31], [32]; linear acceleration). However, we did not eliminate tactile cues because we could not prevent fish from contacting the substrate and our flow rate was sufficient to displace substrate coupled fish along the bottom and against the rear mesh of arena. Therefore, we propose that lateral line

134 ablated fish might have used tactile cues to gain an external frame of reference and perform
135 rheotaxis ([8], [10]), but explicitly testing this idea would require designing an experimental
136 apparatus that enables the video capture of fish movements along the vertical plane (Z-axis),
137 which is not possible in our translucent micro flume.
138
139 *Ototoxic Compounds Differentially Influence the Distribution of Mean Body Angles During Flow*
140 To identify differences in body orientation, the mean body angle for fish in the presence
141 or absence of flow stimuli were compared among treatment groups (Fig. 3). Since flow
142 originated at the top of the flume (located at 0°), mean body angle was determined relative to
143 that of the oncoming water stimulus. The angular variance of each group is represented by the
144 inverse of the mean length of the resultant vector (i.e., short vectors = high variance, and vice
145 versa; Fig. 3). Under no flow, fish from each treatment group swam with a random orientation,
146 indicated by a grand mean body angle that was statistically different from 0° and length of the
147 resultant vector close to zero (Fig. 3a, Supplementary Table 2). When flow was applied, all
148 groups exhibited significant alignment into the oncoming flow stimulus because the grand mean
149 body angles were clustered at 0° and length of the resultant vectors were close to one (Fig. 3b-
150 c).
151 During rheotaxis, post-hoc comparisons within treatment groups showed a significant
152 difference in the homogeneity of distributions between initial and final portions of the flow
153 stimulus, indicating that overall orientation behavior within groups was not consistent for the
154 duration of flow presentation (Fig. 3b-c, Supplementary Table 3). Comparisons among groups
155 within the initial 10s portion of flow showed a significant difference in the distribution of mean
156 body angles between control and $CuSO_4$ fish, and between control and neomycin fish (Fig. 3b,
157 Supplementary Table 3). There was an interaction between treatment and stimulus where the
158 distribution of mean body angle in $CuSO_4$-ablated fish during the initial stimulus bin was different

159 than that of neomycin-ablated fish during the final stimulus bin (Supplementary Table 3),

160 suggesting that these lesion methods differentially impacted the rheotaxis behavior of fish.

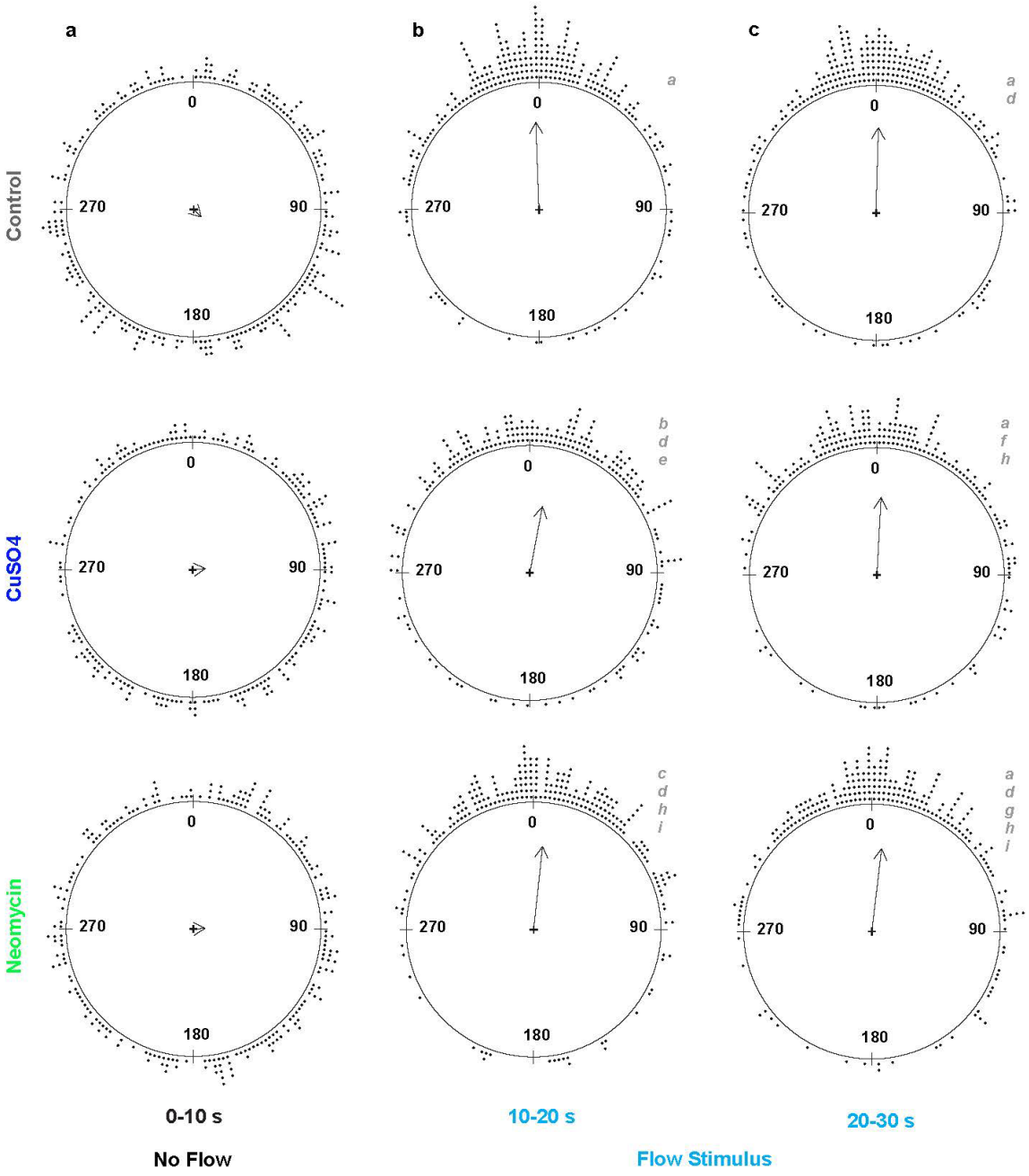

161

162 **Figure 3. The mean resultant vectors of fish treatment groups before and during water flow stimulus indicates fish with**

163 **lateral-line organs ablated by $CuSO_4$ or neomycin can still perform rheotaxis.** Each dot outside the circles represents the mean

164 body angle of an individual fish for the 10 s duration of the no flow and flow stimulus conditions. The grand mean vector for each

group is represented by a summary vector with an angle, *theta*, and a mean resultant length, *rho*, where the length of the vector represents the distribution of individual angles around the mean angle of the group. The length of the vector ranges from zero for uniform distributions, to one for distributions perfectly aligned with the mean angle. Consequently, the angular variance (1- *rho*) is inversely related to vector length. Under no flow (t = 0-10 s), groups of lateral line intact (control, n = 248) and lesioned (CuSO4, n = 204; neomycin, n = 222; 18 experimental sessions) fish have a random distribution of individual mean body angles. Under flow, all groups show a statistically significant orientation to 0° ± 45°, but the distributions of the individual mean angles within the groups differ between the initial (t = 10-20 s) and final (t = 20-30 s) stimulus bins. Distributions with the same lowercase letter indicate groups that do not differ statistically.

Lateral Line-Ablated Fish Performed Rheotaxis for Shorter Durations but Travelled Longer Distances

Although an intact lateral line was not required to perform rheotaxis, lesioned fish behaved differently than non-lesioned fish in flow stimulus, indicating that lack of input from neuromast hair cells affected rheotaxis behavior. To quantify differences in the gross metrics of rheotaxis behavior among groups, we used generalized linear mixed models (GLMMs) that accounted for the random effects of individual variation to compare the mean duration and mean number of rheotaxis events, total distance traveled, and latency between flow presentation and behavior onset. We standardized the data by comparing events of rheotaxis to events when fish were randomly oriented at 0° ± 45° under no flow. Hereafter both conditions are referred to as “events”.

Without flow, the mean duration of random orientation events did not differ among treatment groups (Fig. 4a, Supplementary Table 4). With flow, the mean duration of rheotaxis events increased for each group, and was greatest in the controls, less in neomycin-, and least in $CuSO_4$-treated fish (Fig. 4a, Supplementary Table 4). An interaction between stimulus and treatment was seen during the initial 10s of flow in the $CuSO_4$ treatment cohort, but during the final 10s the differences among all treatments became significant (Supplementary Table 4). Additionally, there was a significant effect of stimulus and an effect of treatment on the mean

192 number of events where the mean was greatest in neomycin-treated, less in controls, and least

193 in $CuSO_4$-treated fish under no flow and flow conditions (Fig. 4b, Supplementary Table 5).

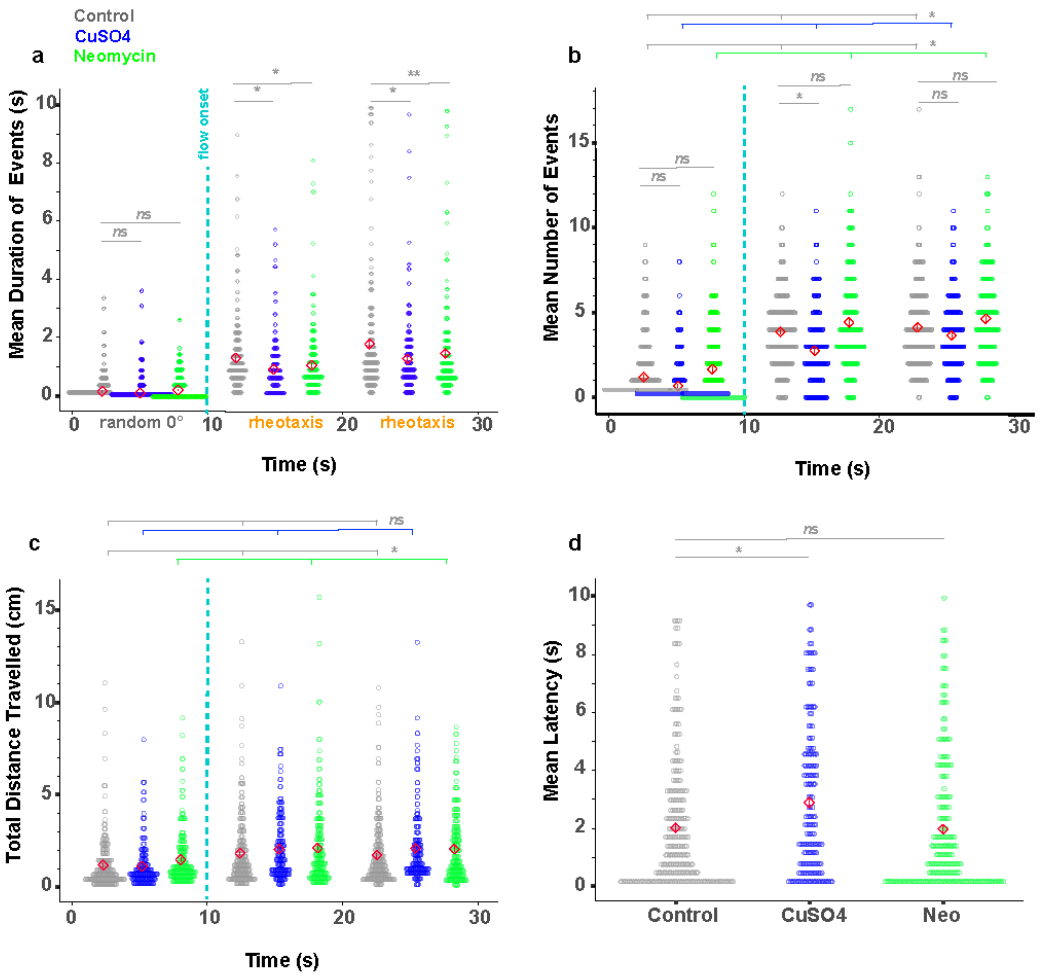

194

195 **Figure 4. Lateral line ablated fish performed rheotaxis for shorter mean durations yet travelled greater total distances**

196 **compared to controls.** Red diamonds in each plot indicate the mean ± SE values. a) Lateral line intact (gray = control, n=248) fish

197 have a longer mean duration of rheotaxis events during flow stimulus than lesioned fish (blue = $CuSO_4$, n = 204; green = neomycin,

198 n = 222; 18 experimental sessions). b) The mean number of 0° orientation and rheotaxis events was greatest for neomycin fish and

199 the least for $CuSO_4$ fish under no flow and flow conditions, respectively. c) Under no flow, neomycin fish traveled a greater total

200 distance than control and $CuSO_4$ fish; but under flow, neomycin and $CuSO_4$ fish traveled a greater total distance than control fish. d)

201 Compared to control and neomycin fish, $CuSO_4$ fish had the longest mean latency to the onset of the first rheotaxis event after flow

202 stimulus presentation. Lines indicate statistical comparisons between control and treatment groups (see Supplementary Tables 4-7).

203 The effects of treatment are indicated by long color-coded bars with branches, whereas interactions are indicated with short bars.

204 There was a significant effect of stimulus in a-c (not shown for clarity). Significance values: * = 0.05, ** = 0.01

205

206 The total distance travelled during events was influenced by the flow stimulus and type of lesion,
207 where neomycin-treated fish travelled further than control and $CuSO_4$-treated fish in the
208 presence and absence of flow (Fig. 4c, Supplementary Table 6). Compared to control and
209 neomycin fish, $CuSO_4$-lesioned fish had a longer latency between flow onset and rheotaxis
210 initiation (Fig. 4d, Supplementary Table S7). Altogether, our data show that an intact lateral line
211 allowed fish to sustain rheotaxis into oncoming flow for longer durations yet travel shorter
212 distances, suggesting that ototoxic compounds reduced the economy of movement of larval
213 zebrafish in response to flow. These results support the idea that the lateral line allows
214 epibenthic fish under flow conditions to hold their station with respect to the substrate ([2], [33])
215 Interestingly, $CuSO_4$ and neomycin ablation affected rheotaxis behavior in different
216 ways. $CuSO_4$ exposure decreased activity, as evidenced by fewer rheotaxis events with greater
217 latency between flow delivery and behavior initiation. This contrasts with the neomycin-exposed
218 fish that exhibited frequent bursts of rheotaxis and travelled longer distances. While zebrafish
219 larvae have been shown to be relatively resistant to the concentration and exposure time of
220 $CuSO_4$ used ([34]), subtle differences in behavior could have been a consequence of nonspecific
221 neural toxicity. Alternatively, the distinct effects of $CuSO_4$ and neomycin treatments on the
222 spatiotemporal nature of rheotaxis might have been due, in part, to their different mechanisms
223 of neuromast ablation. In $CuSO_4$-treated fish, the hair cells were completely ablated, and the
224 supporting cells and afferent neurons were severely damaged ([17]). However, on occasion a few
225 hair cells would remain in neomycin-treated fish (Fig. 2c, f). If residual hair cells in the neomycin
226 group retained some functionality despite severe morphological damage, then it is possible that
227 their sensitivity might have been amplified through efferent modulation ([35]), or influenced by
228 intact supporting cells (Fig. 2c, f) and recruited from a “silent” state (e.g.,[36]), to compensate for
229 reduced sensory input thus resulting in the observed difference in behavior between lesioned
230 groups.

231

232 *Overall Spatial Use of the Arena During Rheotaxis Differs Among Treatments*

233 During flow, we observed that lateral line-lesioned fish were often pushed against the
234 back of the testing arena, whereas intact fish were often swimming at the front of the arena near
235 the flow source. To quantify this observation, density plots of the location of fish in the arena
236 throughout the duration of the experiment were generated (Fig. 5 (2D); Supplementary Fig. 2
237 (1D)) then compared among treatments. The total density of fish in 2D space was parsed out
238 over five regions of interest (ROI, Fig. 5a) that were determined by the size of fish, their
239 orientation during rheotaxis, and the dimensions of the flow field.

240 Under no flow, fish that were placed into the flume generally avoided the middle as they
241 explored the boundaries of the arena; however, $CuSO_4$-treated fish preferred the middle more
242 and explored the boundaries less than the control or neomycin-treated fish (Fig. 5a,
243 Supplementary Fig. 2). Under flow, generalized linear models (Supplementary Table 8) indicate
244 that the spatial use of fish during rheotaxis differed among all three treatment groups. (Fig. 5d).
245 Fish from all treatment groups performed rheotaxis with a pronounced preference for the sides
246 (Fig. 5d) that mimicked the small lateral gradient in the laminar flow field (Supplementary Fig.
247 3a). The reduced velocity of the laminar flow gradient along the sides was created by a minute
248 boundary layer of null flow adjacent to the wall that gradually increased (over ~2-5 mm, front to
249 rear) until it became part of the freestream flow field (i.e., blue arrows in Supplementary Fig. 3).
250 The gradient provided a refuge (e.g., [37]) where intact and lesioned fish could swim into the flow
251 with reduced energetic cost ([38]). As our definition of rheotaxis (see methods; Supplementary
252 Fig. 1d, e) specifies that only fish that moved their tail and had forward body translation into the
253 flow, fish that were in null water flow (i.e. too close to the wall) were excluded from the rheotaxis
254 dataset. Furthermore, control fish frequently performed rheotaxis while maintaining position in
255

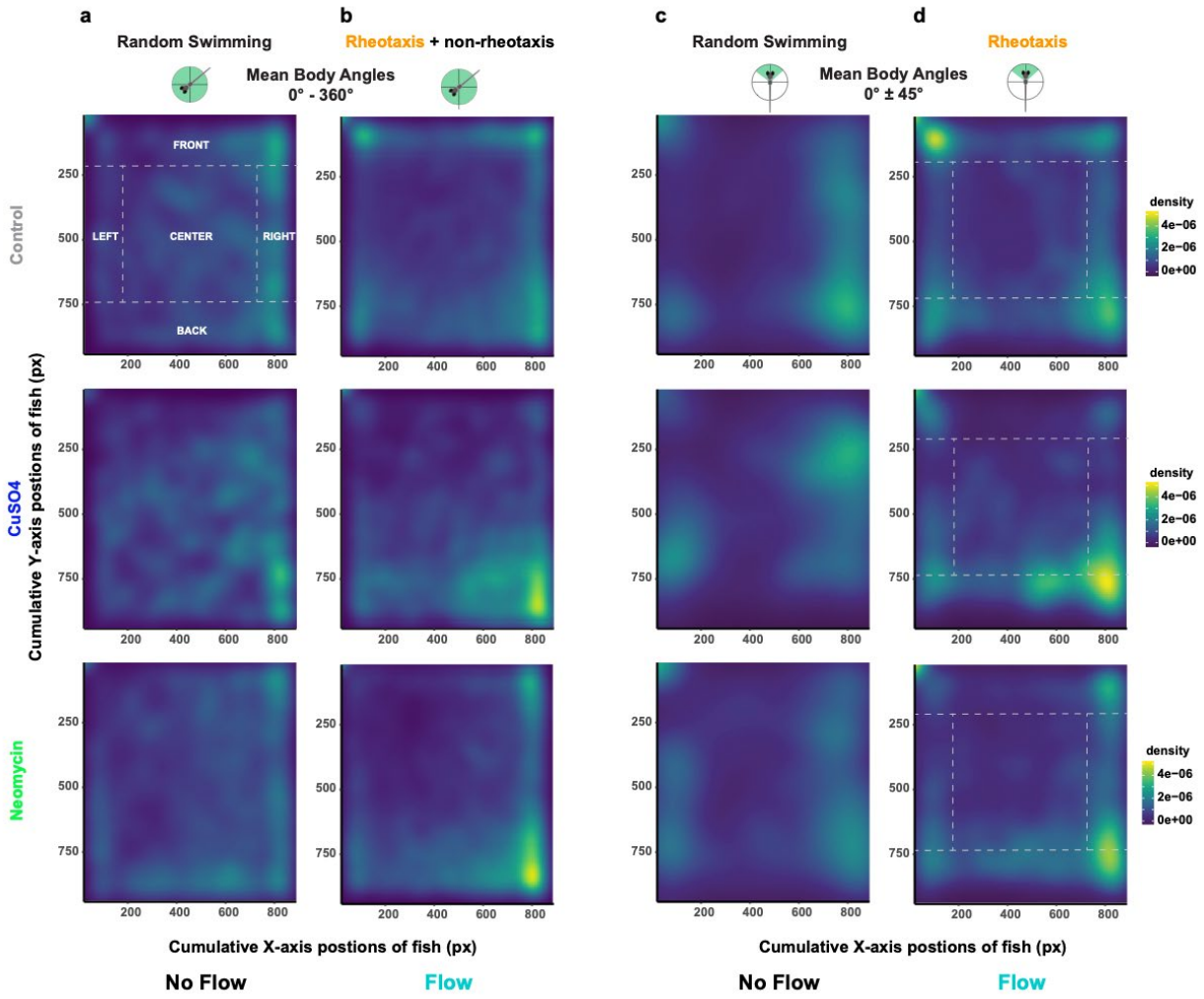

Figure 5. Under flow, lateral line intact (control) fish used the front part of the arena near the source of the flow, whereas lesioned (CuSO4, neomycin) fish use the back portion of the arena. a-b) For all possible mean body angles (0°- 360°): a) all treatment groups of fish show similar density, or total spatial use, of the arena under no flow conditions; b) however, the controls (control, n = 248) used the front of the arena and the lesioned (CuSO4, n = 204; neomycin, n = 222; 18 experimental sessions) fish used the back of the arena under flow. c-d) Filtering the data for mean body angles required for rheotaxis (0° ± 45°): c) all groups clustered along the left and right sides of the arena under no flow; d) but under flow, the controls used the front-left and the lesioned use the back-right portions of the arena. Dotted lines and labels in capital letters indicate spatial regions of interest (ROI). For clarity, statistical comparisons among treatment and ROIs were not included in the figure; however, there were significant fixed effects for CuSO4 and neomycin treatments, the back ROI, and interactions between treatment and ROI (Supplementary Table 8).

the flow near the upper-left corner of the arena whereas lesioned fish primarily occupied the back-right corner (Fig. 5d, Supplementary Fig. 3b). These observations indicate that an intact

269 lateral line enabled larval zebrafish to better station hold while occupying the areas of strongest
270 flow (Supplementary Fig. 3b) and avoid being swept backwards against the rear mesh. The
271 propensity of lesioned fish to use the rear of the arena while performing rheotaxis in the
272 absence of visual ([3]) and horizontal vestibular ([31], [32]) cues suggests that these larvae might
273 have used tactile cues to provide the external frame of reference necessary to orient and swim
274 against flow ([2], [8], [10]). Unfortunately, our flume design and camera setup prevented us from
275 exploring this possibility.
276
277 *Lateral Line Ablation Reduces the Proportion of Individual Fish that Perform Rheotaxis*
278 During flow presentation, the control group had the greatest proportion of individual fish
279 that performed rheotaxis during the experiment (as defined in Supplementary Fig. 1) followed by
280 neomycin-treated then $CuSO_4$-treated groups (Fig. 6). Intact fish plateaued relatively quickly
281 compared to lesioned fish, but the values for all three groups converged during the final few
282 seconds of flow presentation.

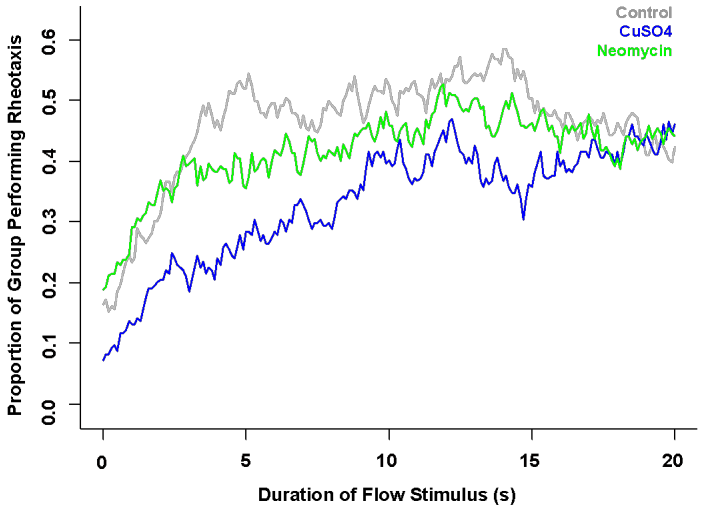

283
284 **Figure 6. Intact lateral line enabled a greater proportion of fish to perform rheotaxis within the first 15 seconds of stimulus**
285 **onset.** Time series of the proportion of individual fish within each group that performed rheotaxis during flow presentation. A greater

286 proportion of lateral line intact (gray = control, n = 248) fish performed rheotaxis than lesioned (blue = $CuSO_4$, n = 204; green =
287 neomycin, n = 222; 18 experimental sessions) fish. The data for all treatments converges after 17 s of flow presentation.
288

289 *Spectral Decomposition Shows that Lateral Line Ablation Impacts the Overall Trend and*
290 *Periodic Fluctuation in Linear and Angular Movement*

291 To uncover the impact that lateral line ablation had on the swimming kinematics of fish,
292 we analyzed how the magnitude of the linear (relative distanced moved, relative velocity,
293 relative acceleration) and angular (mean body angle, mean length of the resultant vector)
294 components of movement changed over time. We observed that all treatment groups swam in
295 the burst-and-glide style that is characteristic of larval zebrafish with intact lateral lines, but with
296 noticeable differences in the quality of their movement. Because the lateral line mediates station
297 holding behavior ([2], [33], [38]), we postulated that, under flow, the oscillations in relative linear and
298 angular movements for lateral line-intact fish would be smaller in magnitude than those of
299 lesioned fish. The observed time series data (Fig. 7a, d, g; Supplementary Fig. 4a, d) had a
300 "seismic" appearance where noise masked the underlying signal. Therefore, we removed the
301 random noise (Supplementary Fig. 4g-k) and decomposed the observed datasets into their
302 fundamental large- and small-scale components: the overall trend in movement magnitude
303 during the entire experiment (Fig. 7b, e, h; Supplementary Fig. 4b, e) and the periodicity, or
304 recurring fluctuations in movement magnitude, that occurred during any given second of the
305 experiment (Fig. 7c, f, i). Because the relative movement (Fig. 7), velocity and acceleration
306 (Supplementary Fig. 4c, f) data showed similar periodic fluctuations, only relative movement is
307 shown in Fig. 7 for visual clarity.

308 During rheotaxis, the trend among groups was that $CuSO_4$ ablation reduced the
309 magnitude of relative movement (Fig. 7b) but not the relative velocity or acceleration of fish
310 (Supplementary Fig. 4c, f) compared to control and neomycin groups. $CuSO_4$- and neomycin-
311 treated fish had a trend of reduced ability to achieve and maintain orientation within flow relative

to controls (Fig. 7e). Lesioned fish had mean resultant vectors (*rho*) of longer length meaning that they had less variance (1- *rho*) in their mean body angle compared to controls (Fig. 7h). These data suggest that an intact lateral line allowed control fish to better detect changes in water flow, regularly make small magnitude course corrections to their body angle (Fig. 7h), rapidly orient into flow with greater accuracy (Fig. 7e), which resulted in a greater proportion of non-lesioned fish performing rheotaxis compared to lesioned fish (Fig. 6).

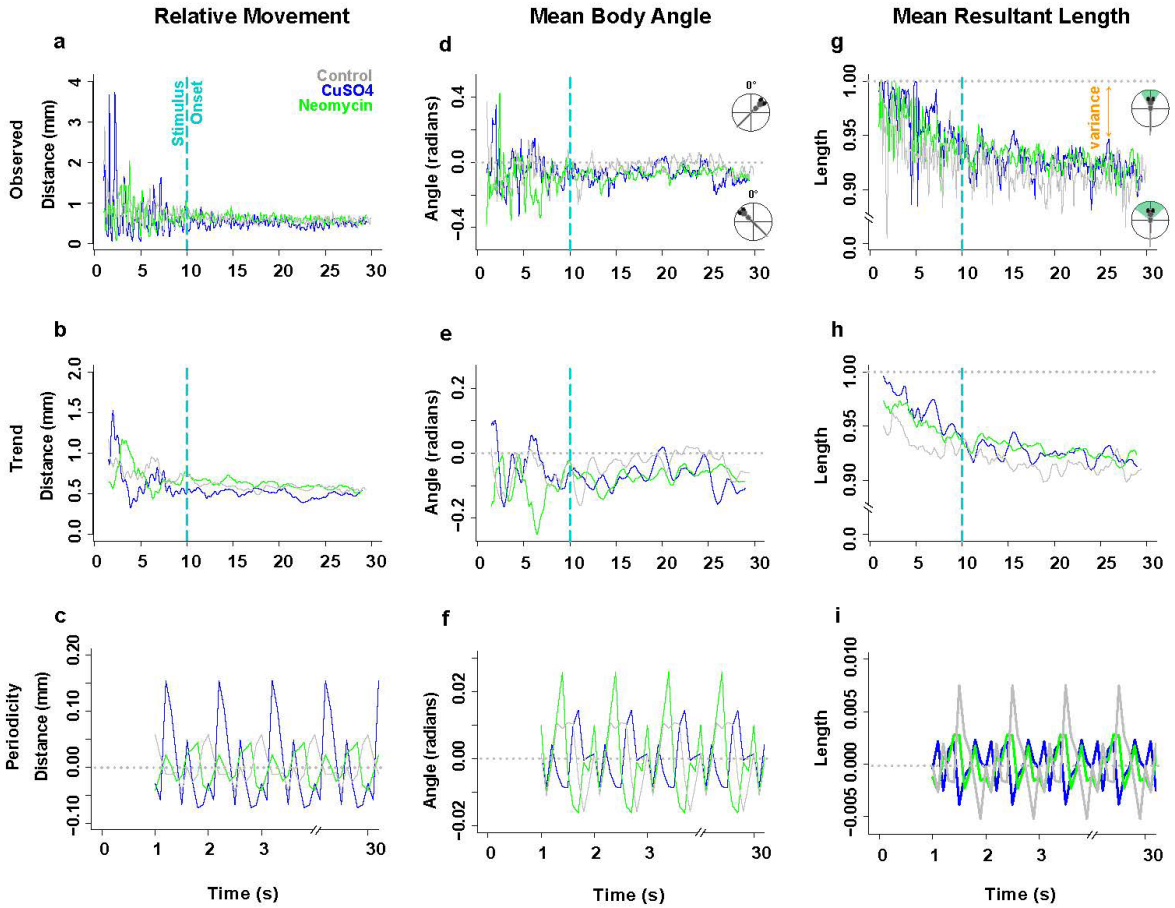

Figure 7. The overall trends and periodic fluctuations in the linear (relative distance moved) and angular (mean body angle, mean length of the resultant vector) motion parameters of rheotaxis behavior differ among treatment groups. (Note: the relative velocity and acceleration periodicity data mimicked the patterns observed in relative movement; see Supplementary Fig. 3). Gray = control (n = 248), blue = $CuSO_4$ (n = 204), green = neomycin (n = 222). Spectral decomposition of the observed data (a, d, g) removed the noise (Supplementary Fig. 3g, h, i) to reveal the overall underlying trends (b, e, h) and the periodicity, or recurring

fluctuations (c, f, i) that occurred during any given 1 s of the experiment. The periodicity waveform peaks (c, f, i) indicate the average amount (amplitude), number, direction (positive = increasing; negative = decreasing), and order of occurrence for these cyclic fluctuations as a function of unit time (1 s). The overall trends were that $CuSO_4$ treated fish had the least relative movement (b), while the control fish more rapidly oriented to 0° (e) and swam with more angular variance (h; 1 – mean length of the resultant vector) compared to lesioned fish. The periodic fluctuation in relative distance moved (c) was greatest in $CuSO_4$ treated fish compared to control or neomycin treated fish. However, the fluctuation in mean body angle (f) was greatest in neomycin treated fish compared to control and $CuSO_4$ fish, while the fluctuation in mean length of the resultant vector (i.e the angular variance; i) was greatest in control fish compared to lesioned fish.

Among treatment groups, there were clear differences in the magnitude of changes in the periodic cycles of linear (Fig. 7c; Supplementary Fig. 4c, f) and angular (Fig. 7f, i) movements during rheotaxis. The linear data show that $CuSO_4$-treated fish had fluctuations of the greatest magnitude in relative distance moved, velocity, and acceleration compared to those of control and neomycin-treated fish (Fig. 7c; Supplementary Fig. 4c, f; Supplementary Table 9). In $CuSO_4$-treated fish, the amplitude of the waveform peaks during the sampling period was large and decreased rapidly, but in control and neomycin-treated fish the peaks were small and increased gradually (Fig. 7c; Supplementary Fig. 4c, f). The large fluctuations of $CuSO_4$-treated fish could serve to compensate for their delayed response to flow (Fig. 4d), but when their trend of lesser relative movement (Fig. 7b) is considered, it results in the greatest relative increase in distance traveled among groups (Fig. 4c). These empirical data support the qualitative observations that $CuSO_4$-treated fish performed rheotaxis with delayed responses and erratic linear movements, whereas control and neomycin-ablated fish performed rheotaxis with low latency responses and graded linear movements.

The periodic fluctuation in mean body angle among treatment groups showed an initial small turn to the left (negative values) followed by a series of right (positive values) and left turns that were of relatively small magnitude in controls and $CuSO_4$-treated fish, and relatively large magnitude in neomycin-treated fish (Fig. 7f; Supplementary Table 9). The amplitude of the waveform peaks in control and $CuSO_4$-treated fish were relatively small and gradually increased

353 during the sampling period, but those of neomycin-treated fish were relatively large throughout.
354 Therefore, control and $CuSO_4$-treated fish performed rheotaxis with a graded response in mean
355 body angle, but neomycin-treated fish performed rheotaxis with large erratic changes in mean
356 body angle. We also examined the periodicity in mean resultant length, which reflects the
357 fluctuation in angular variance as fish performed rheotaxis. In control fish, the waveform had
358 peaks of small amplitude that rapidly increased during the sampling period, but in lesioned fish
359 the waveform was comprised of small peaks of consistent amplitude (Fig. 7i). Intact fish showed
360 a graded response where small initial changes in angular variance preceded much larger
361 subsequent changes that coincided with the flat portion of the peaks in mean body angle (Fig.
362 7f), which indicates that control fish regularly made small changes in their body angle and
363 maintained this new heading before making another angular adjustment. Conversely, lesioned
364 fish had very little fluctuation in angular variance (Fig. 7i) once a mean body angle was chosen,
365 regardless of whether the change in mean body angle was relatively small (e.g., $CuSO_4$) or
366 large (e.g., neomycin; Fig. 7f).
367 These data support that, during rheotaxis, fish with an intact lateral line organ made
368 small adjustments to their linear movement, velocity, acceleration, and mean body angle with a
369 high degree of variability. This graded, flexible, and finely tuned behavioral response to flow
370 resulted in a greater ability of control fish to rapidly attune and maintain fidelity to the oncoming
371 flow vector (Fig. 7e). Conversely, $CuSO_4$- and neomycin-ablation caused fish to swim into flow
372 with erratic linear and angular movements, respectively, which ultimately undermined their
373 ability to maintain a 0° heading into the flow (Fig. 7e).
374
375 *Spectral Analysis Reveals that Lateral Line Ablation Impacts the Temporal Fluctuation of Linear*
376 *and Angular Movement*
377 To determine the impact that lateral line ablation had on the frequency of the fluctuations
378 in linear and angular movement, we decomposed each periodicity dataset (Fig. 7c, f, i;

379 Supplementary Fig. 4c, f) into a power spectrum that depicted the spectral density (i.e., number
380 of changes in movement per frequency) over a continuous range of frequencies (Fig. 8a-e). For
381 each parameter, the frequency and amplitude of three most dominant peaks were summed to
382 calculate the net shifts in frequency and spectral density among treatment groups
383 (Supplementary Table 10). Relative to controls, the power spectra of $CuSO_4$- and neomycin-
384 treated fish showed a net shift to lower dominant frequencies (downshift) and a net increase in
385 the density of the dominant peaks for relative movement, velocity, and acceleration (Fig. 8a-c,
386 Supplementary Table 10), which indicates that lateral line-ablated fish performed rheotaxis with
387 greater numbers of linear movements to compensate for their overall reduction in fluctuation
388 frequency. The rheotaxis behavior of $CuSO_4$-treated fish showed less frequent fluctuations in
389 relative movement compared to controls and neomycin-treated fish (Fig 8a), but the fluctuations
390 in relative velocity and acceleration for $CuSO_4$-treated fish and controls occurred over a wider
391 range of frequencies than those of neomycin-treated fish (Fig 8b-c). Specifically, the relative
392 movement spectra of the control and $CuSO_4$-treated fish had broad clusters of dominant peaks
393 that gradually shifted to higher frequencies (upshifted) for relative velocity and acceleration.
394 However, the spectra of neomycin-treated fish were dominated by a single high-density peak
395 that consistently occurred at 0.21 Hz for relative movement, velocity, and acceleration (Fig. 8a-
396 c). These data reveal that lateral line ablation results in rheotaxis behavior characterized by
397 fluctuations in relative movement, velocity and acceleration that occur less frequently, but that
398 neomycin ablation has the additional effect of “temporally restricting” the frequency of
399 fluctuations in linear movement to occur around a consistent dominant frequency.
400 Power spectra density curves indicated that intact fish performed rheotaxis with fewer
401 numbers of fluctuations in mean body angle that occurred less frequently, whereas lesioned fish
402 performed rheotaxis with a greater numbers of high frequency fluctuations in mean body angle.
403 The spectrum of controls shows five broadly spaced peaks, but those of the lesioned fish have
404 fewer peaks that are clustered around the dominant frequencies (Fig. 8e) indicating that intact

405 fish performed rheotaxis with greater variety in the frequency of fluctuations in their angular
406 variance compared to lesioned fish (Fig. 8e). We observed the mean body angle of $CuSO_4$- and
407 neomycin-treated fish showed a net upshift in the dominant frequencies, a net increase in
408 dominant peak density, and temporal restriction, or greater clustering of power spectra into
409 distinct peaks, relative to that of controls (Fig. 8d, Supplementary Table 10). By contrast, the
410 spectrum of control fish was relatively flat with low density peaks that lacked distinct clustering
411 into dominant frequencies (Fig. 8d) Additionally, there were two divergent patterns seen in the
412 power spectra for mean resultant vector length in lesioned fish: $CuSO_4$-treated fish had a net
413 downshift in dominant frequencies and a net increase in peak density, whereas neomycin-
414 treated fish had a net upshift in frequency and a net decrease in peak density relative to those
415 of controls (Fig. 8e, Supplementary Table 10). Thus, $CuSO_4$-lesioned fish performed rheotaxis
416 with greater number of fluctuations in angular variance that occurred less frequently, but
417 neomycin-lesioned fish performed rheotaxis with fewer numbers of fluctuations in angular
418 variance that occurred more frequently compared to intact fish. These results show that lateral
419 line ablation in larval zebrafish resulted in rheotaxis behavior with greater numbers of
420 fluctuations in mean body angle, fewer numbers of fluctuations in angular variance, and a
421 greater clustering of angular movements into fewer peaks.
422

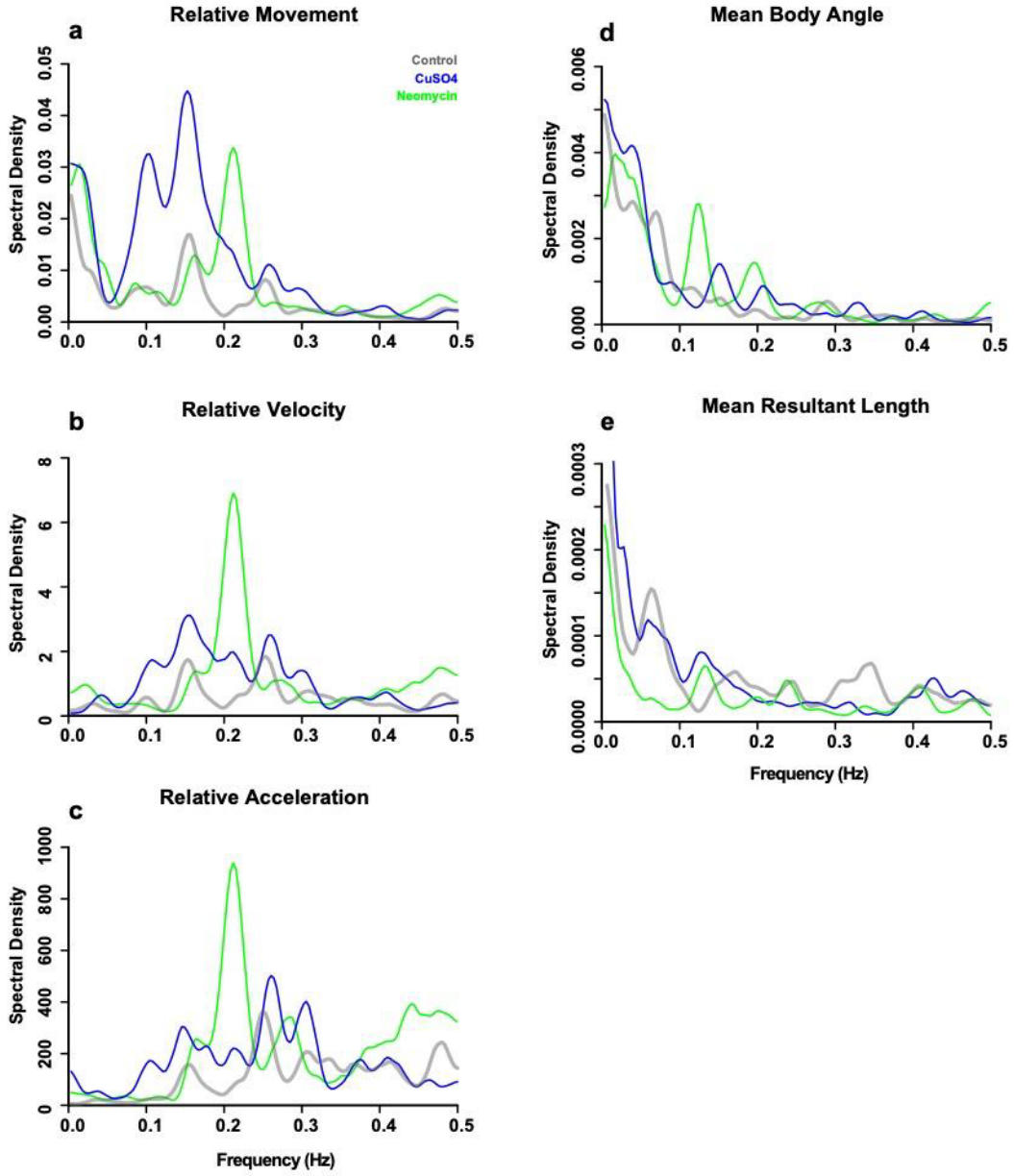

Figure 8. Power spectra density curves show that an intact lateral line allowed fish to make fewer yet more temporally variable changes in relative linear and angular movement. Because frequency and period are inversely related, the low frequency peaks to left of the periodograms indicate cycles with longer periods, and vice versa The amplitude of the peaks indicates the spectral density, or the number of movement events at a given frequency that occurred during the experiment. The peaks with the greatest amplitude indicate the fundamental or dominant frequencies of fluctuation in the periodicity data. The frequency and amplitude of three most dominant peaks were summed to calculate the net shifts in frequency and power. Relative to controls (gray, n =248), lesioned (blue = $CuSO_4$, n=204; green = neomycin, n = 222) fish had a net downshift in the three dominant frequencies of (a) relative movement, (b) velocity, and (c) acceleration and a net upshift in (d) mean body angle of larval zebrafish during rheotaxis.

For the dominant frequencies of (e) mean resultant length, there was a net downshift and upshift for $CuSO_4$- and neomycin-treated fish, respectively. Furthermore, relative to lateral line intact fish, the peaks of lesioned fish are clustered into fewer peaks of greater amplitude over a relatively narrow range, which indicates that lateral line ablation increased the number yet reduced the temporal variation of changes in movement.

We interpret the relatively flat and low-density power spectra observed in control fish (Fig. 8a-d) to indicate that an intact lateral line allowed fish to respond to flow with fewer overall fluctuations in linear and angular movement over a broader range of fluctuation frequencies compared to lesioned fish. It is sensible that the mechanosensory input from lateral line hair cells gave intact fish a greater ability to respond to flow with greater efficiency, efficacy, and economy of movement. Conversely, fewer peaks of greater density observed in lateral line lesioned fish indicates that losing the ability to detect water flow led to more changes in linear or angular movement that occurred over a restricted range of frequencies thus reducing the effectiveness of their movements in response to flow.

Cross Correlation Between Linear and Angular Movements Shows Distinct Rheotaxis Profiles Among Groups

In the absence of visual cues, intact larval zebrafish detected the presence of flow through a change in linear or angular displacement ([22]) and responded by either turning right, left, or moving forward into the flow. Because these movements relied on input from the lateral line, we investigated the effect of ototoxic compounds on the cross correlation between linear and angular movements. The correlograms depict the degree, direction, and relative timing between an above average increase in relative movement (Fig. 9a-b), velocity (Fig. 9c-d), or acceleration (Fig. 9e-f) and an above average change in mean body angle (Fig. 9a, c, e) or mean resultant length (Fig. 9b, d, f). By focusing on the strongest cross-correlations, treatment-specific patterns emerged in the direction and relative timing between large changes in linear and angular movements during rheotaxis.

459 The rheotaxis movements of control fish in response to flow were smoother, less erratic,
460 and more effective at station holding within the flow field compared to those of lesioned fish. The
461 rheotaxis profile of control fish was such that the relative timing and direction of changes in
462 mean body angle depended upon the time derivative of the linear movement, but changes
463 angular variance were consistent across all linear movements. For example, intact fish tended
464 to change their mean body angle to the *left* of flow *before* a large change in relative movement
465 (Fig. 9a), to the *right* of flow *simultaneous* with changes in velocity (Fig. 9c), and to the *left* of
466 flow *after* changes in acceleration (Fig. 9e). However, the strongest correlation between a
467 *reduction* in angular variance always occurred *prior* to large changes in relative movement (Fig.
468 9a), velocity (Fig. 9c), and acceleration (Fig. 9e). In lesioned fish, the timing and direction of the
469 strongest cross-correlations shifted the rheotaxis profile of these fish away from that of controls
470 in a predictable, consistent, and treatment-specific manner. $CuSO_4$-treated fish tended to
471 change their mean body angle to the *right* of the oncoming flow vector *after* large changes in
472 movement (Fig. 9a), velocity (Fig. 9c), and acceleration (Fig. 9e). However, neomycin-treated
473 fish tended to change their body angle to the *left* of the flow *after* changes in movement (Fig.
474 9a), velocity (Fig. 9c), and acceleration (Fig. 9e). As in controls, lesioned fish always had a
475 *reduced* angular variance correlated with changes in their linear movements, but the relative
476 timing of the cross correlation shifted according to the ototoxic compound used and the time
477 derivative of the linear movement. In $CuSO_4$-treated fish, the strongest correlation between a
478 *reduction* in angular variance tended to occur *prior* to changes in movement (Fig. 9b), and *after*
479 changes in velocity (Fig. 9d) or acceleration (Fig. 9f). Conversely, in neomycin-treated fish,
480 *reductions* in angular variance occurred *after* changes in movement (Fig. 9b), and *before*
481 changes in velocity (Fig. 9d) or acceleration (Fig. 9). These data revealed that control fish with
482 an intact lateral line detected oncoming flow and adjusted their mean body angle *prior* to
483

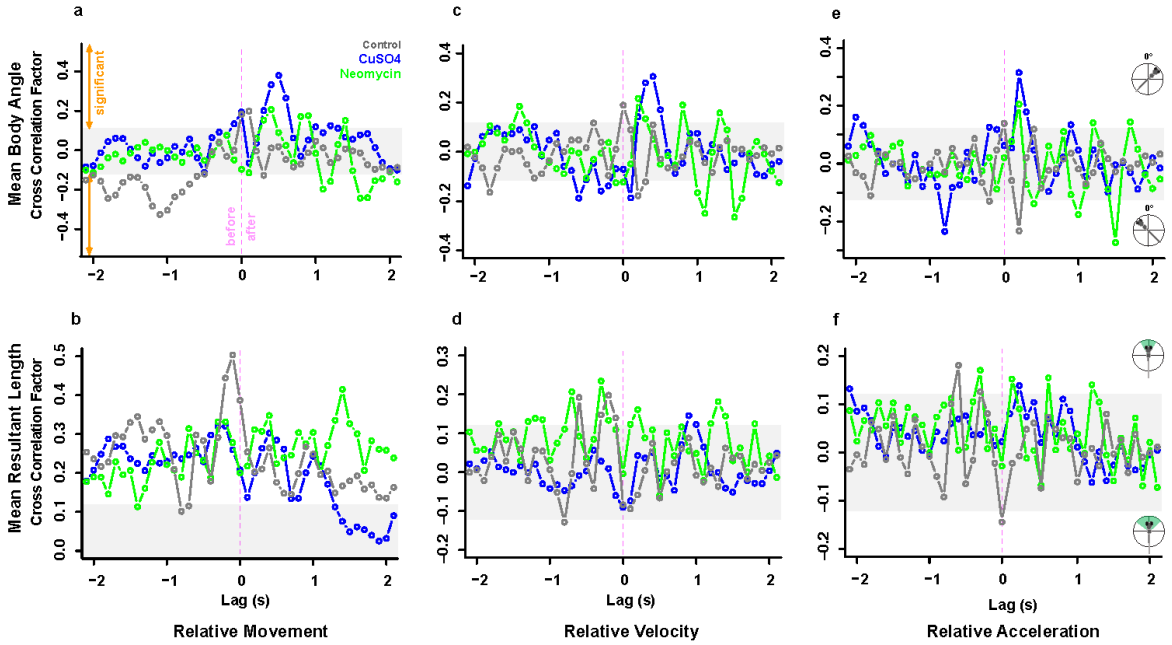

Figure 9. Cross correlations between linear and angular movement data indicate ototoxic compound-specific changes to the rheotaxis behavioral profile of fish. The correlograms depict how an above average increase in relative movement (a, b), relative velocity (c, d), or relative acceleration (e, f) were significantly cross correlated with above average increases or decreases in the mean body angle (a, c, e) or mean resultant length (b, d, f). In the figures for mean body angle (a,c,e), the positive and negative peaks indicate that fish were oriented to the right or left of the oncoming flow vector, respectively. In the figures for mean resultant length (b, d, f), the positive and negative peaks indicate fish that had a lesser or greater variance of the mean body angle, respectively. The X-axis indicates the relative timing, or lag, of the cross correlation between the angular parameter with respect to an above average increase in the linear parameter (zero = simultaneous occurrence; negative = angular change occurs *before* linear change; and positive = angular change occurs *after* linear change). *For example, interpret panel 10a as:* In control (gray, n = 248) fish, above average increases in relative movement are significantly correlated with changes in mean body angle to the left of the flow vector that previously occurred. In $CuSO_4$-treated (blue, n =204) fish, above average increases in relative movement are significantly correlated with above average changes in mean body angle that subsequently occurred. In neomycin-treated (green, n = 222) fish, above average increases in relative movement are significantly correlated with below average changes in mean body angle that subsequently occurred.

making a change in their relative movement, while lateral line lesioned fish changed their mean body angle *after* a change in their relative linear movement. Our results support the reported mechanism of water flow detection in larval zebrafish where they use their lateral line hair cells

503 to sense the vorticity, or curl, created by gradients in the flow field the determine flow direction
504 by measuring the temporal change in vorticity as they experience flow ([22]).
505 It appears that an intact lateral line allowed fish to rapidly detect flow and adjust their
506 heading prior to swimming into the flow. However, in the absence of lateral line and visual cues,
507 and the inability of 6-7dpf zebrafish larvae to detect horizontal angular cues (yaw) by the
508 vestibular system ([31], [32]), it is possible that lesioned fish might have relied on tactile cues, such
509 as physical displacement along the substrate, to gain an external frame of reference necessary
510 to orient and swim into flow. Intact fish also tended to change their body angle to the left of the
511 flow vector, which may reflect lateral line handedness where larval zebrafish prefer to use the
512 left side of their lateral line to detect flow stimuli in a manner like that of blind cavefish ([39]).
513 Lateral line ablation shifted the relative timing of the cross correlations between angular and
514 linear movement and might have impaired any potential lateral line handedness, which may
515 have further contributed to the erratic rheotaxis behavior observed in lesioned fish.
516 In summary, lateral line ablation of larval zebrafish resulted in distinct, treatment-specific
517 rheotaxis profiles that differed from that of intact fish in the following ways: 1) delayed relative
518 timing between changes in mean body angle and all linear movements, 2) changed mean body
519 angle in response to flow, and 3) shifted timing between reductions in angular variance and
520 changes in linear movement.
521
522 **CONCLUSIONS**
523 In this study, ablating the lateral line of larval zebrafish with two commonly used ototoxic
524 compounds impacted their ability to produce the fine adjustments required to station hold in
525 response to water flow. Lateral line ablation inhibited the ability of fish to discriminate subtle
526 distinctions in flow, resulting in more intense overcorrections and decreased economy of motion.
527 Our data support the hypotheses that the lateral line mediates station holding behavior ([2], [33], [38]),
528 but is not required for rheotaxis behavior ([2], [11], [12], [29], [30]) in larval zebrafish in non-uniform laminar

529 flow. We posit that the physical displacement of lesioned fish along the substrate may have
530 provided sufficient tactile cues ([8], [10]) necessary for lateral line ablated fish to perform rheotaxis.
531 We propose that the greater angular variance observed in intact fish might indicate that
532 these fish were regularly sampling the velocity gradients of the flow stimuli ([22]) from a variety of
533 body angles so that they could reduce their response latency, quickly orient with respect to
534 fluctuating flow stimuli, and maintain their overall mean body angle with greater fidelity to the
535 flow vector than lesioned fish. During flow, intact fish had recurring fluctuations in relative
536 movement, velocity, and mean body of lower magnitude, and fluctuations in relative movement,
537 velocity, acceleration, and mean body angle of controls that were fewer in number yet occurred
538 over a wider range of temporal frequencies compared to lesioned fish. Thus, the sensory cues
539 detected by the lateral line allowed control fish to respond to water flow with less intensity and
540 greater temporal variation in their movements, resulting in greater economy of movement.
541 This is the first study to demonstrate that two ototoxic compounds commonly used to
542 ablate the lateral line impacts the behavioral profiles and mechanism of rheotaxis in zebrafish.
543 We propose a novel functional assay for understanding the behavioral impacts of sensory hair
544 cell ototoxicity, which may be used to supplement future studies exploring lateral line injury,
545 protection, and recovery. Furthermore, the simplicity of the equipment and precision of the
546 machine learning analyses used in this assay make it amenable to adaptation for detecting
547 subtle behavioral changes in a wide variety of animal models.
548
549 **METHODS**
550 *Ethics Statement*
551 This study was performed with the approval of the Institutional Animal Care and Use
552 Committee of Washington University School of Medicine in St. Louis and in accordance with
553 NIH guidelines for use of zebrafish.

554

555 *Zebrafish*

556 Adult zebrafish were raised under standard conditions at 27-29°C in the Washington
557 University Zebrafish Facility. The wild type line AB* was used for all experiments unless
558 otherwise stated. Embryos were raised in incubators at 28°C in E3 media (5 mM NaCl, 0.17 mM
559 KCl, 0.33 mM $CaCl_2$, 0.33 mM $MgCl_2$; ([40])) with a 14:10 hr light:dark cycle. After 4 days post
560 fertilization (dpf), larvae were raised in 100-200 mL E3 media in 250-mL plastic beakers and fed
561 rotifers daily. Sex was not considered because it cannot be determined in zebrafish larvae at the
562 developmental stage used in this study.

563

564 *Lateral Line Ablation*

565 At 6 or 7dpf, ~15 larval zebrafish were placed into each well of a flat bottom 6-well
566 polystyrene plate (#351146, Falcon) in 8 mL of E3 media. Treatment animals were placed into
567 50 μM neomycin trisulfate salt hydrate (N1876-25G, Sigma Aldrich) or 10 μM $CuSO_4$ (451657-
568 10G, Sigma Aldrich) solutions made in 8 mL of E3 media. The concentration of neomycin used
569 (50 μM) was chosen to introduce the maximum amount of lateral line hair cell loss with minimal
570 damage to muscle fibers ([41]). The plate was placed into an incubator at 29°C and exposed to
571 the treatment for 30 min (neomycin) or 60 min ($CuSO_4$). After exposure, the fish were removed
572 from treatment, rinsed 3X in media, placed into 8 mL of clean media and allowed to recover in
573 the incubator for 120 min ($CuSO_4$) or 150 min (neomycin) to standardize the total experimental
574 time to 180 min. Control fish received no chemical treatments yet underwent the same
575 procedures as the $CuSO_4$ and neomycin fish. At the end of treatment, the larvae were removed
576 from the incubator and immediately began rheotaxis behavior trials.

577

578 *Immunohistochemistry*

579 Lateral line ablation was confirmed via immunohistochemistry on a subset of control and
580 lesioned fish used in the behavior experiments. Larvae were sedated on ice (5 min, 0°C) then
581 fixed overnight at 4°C in PO_4 buffer with 4% paraformaldehyde, 4% sucrose, and 0.2 mM $CaCl_2$.
582 Larvae were rinsed 3X with PBS and blocked for 2 hr at room temperature in PBS buffer with
583 5% horse serum, 1% Triton-X, and 1% DMSO. Primary antibodies for Otoferlin (HCS-1, mouse
584 IgG2a, 1:500, Developmental Studies Hybridoma Bank,) and Calbindin (mouse IgG1, 1:1000,
585 Cat#:214011, Synaptic Systems) were diluted in 1x PBS buffer with 2% horse serum and 0.1%
586 Triton-X, then incubated with the larvae overnight at 4°C with rotation. Larvae were rinsed 5X
587 with PBS solution, then placed in secondary antibody (goat anti-mouse IgG2a, Alexa 488,
588 1:1000, ThermoFisher; goat anti-mouse IgG1, Alexa 647, 1:1000, ThermoFisher) diluted in PBS
589 with 2% horse serum and incubated for 2 hr at 22°C with rotation. Fish were rinsed 3X with PBS
590 then incubated with DAPI (1:2000, Invitrogen) in PBS for 20 min at 22°C to label cell nuclei.
591 Larvae were rinsed 2X with PBS then mounted onto glass slides with elvanol (13% w/v polyvinyl
592 alcohol, 33% w/v glycerol, 1% w/v DABCO (1,4 diazobicylo[2,2,2] octane) in 0.2 M Tris, pH 8.5)
593 and #1.5 cover slips.
594

595 *Confocal Imaging and Hair Cell Quantification*

596 Immunolabeled z-stack images were acquired via an ORCA-Flash 4.0 V3 camera
597 (Hamamatsu) using a Leica DM6 Fixed Stage microscope with an X-Light V2TP spinning disc
598 confocal (60 µm pinholes) controlled by Metamorph software. The region of interest tool in
599 Metamorph was used to select specific neuromasts (~700 x 700 px) from the surrounding area.
600 Z-stack images of 100 ms exposure were acquired through a 63X/1.4 N.A. oil immersion lens,
601 0.5 µm z-step size. Excitation for DAPI (405 nm) Alexa 488, and Alexa 647 was provided by
602 89 North LDI-7 Laser Diode Illuminator on the lowest power setting (20%) that could acquire
603 images and minimize photobleaching. Confocal images were processed in FIJI (ImageJ, NIH)

604 software to create maximal intensity z-stack projections with minor exposure and contrast
605 adjustments. Hair cells were quantified by scrolling through z-stacks and counting only cells that
606 had both DAPI and HCS-1 labels present. Any hair cells that had pyknotic nuclei (indicated by
607 condensed DAPI labeling) were not included in the counts. For each fish, the mean number of
608 hair cells per neuromast for the midline was calculated among multiple locations (L3-5), and for
609 the supra orbital (SO1, SO2) neuromasts the mean was calculated between the left and right
610 locations to account for interindividual variation. Hair cell count distributions were tested for
611 normality; statistical significance was determined using the Kruskal-Wallis test with Dunn's
612 multiple comparisons post hoc tests using GraphPad Prism 9.2.0.
613
614 *Experimental Apparatus for Rheotaxis Behavior*
615 A microflume (220 x 100 x 40 mm; Fig. 1a) was constructed in two pieces of translucent
616 clear resin (RS-F2-GPCL-04, Formlabs) using a high-resolution 3D printer (Form 2, Formlabs)
617 and joined with two-stage epoxy. Flow collimators (~40mm long) made of ~3mm diameter
618 plastic straws were placed immediately upstream of the working section in a portion of the flume
619 bounded on either side by plastic mesh (25 μm) that was cemented to the wall with epoxy (Fig.
620 1a). Silicone sealant was used to cement a 1 mm-thick layer of plastic on top of flume to prevent
621 water spillage from the high-pressure side of the flume by covering the pump outflow, first bend,
622 and flow collimators up to the working section. The low-pressure portion of the flume
623 downstream from the working section was open at the top to facilitate the addition and removal
624 of larval zebrafish and water when necessary. Larvae were isolated within the upper 10 mm of
625 the flume working section to enable reliable video recording by a square (30 x 30 x 10 mm)
626 arena that was 3D printed from clear resin. Plastic mesh (25 μm) was cemented with epoxy to
627 the upstream and downstream sides of the removable arena which allowed water to flow
628 through the working section after the arena was friction seated into the channel at the top of the
629 flume and immediately adjacent to the flow collimators. An Arduino (UNO R3, Osepp) with a

digital display used custom scripts to control the onset and offset of the pump and camera to ensure the consistent duration of water flow and video recordings. Flow of constant velocity was provided by a 6V bow thruster motor (#108-01, Raboesch) inserted into the flume (Fig. 1b) and modulated by an inline rheostat between the Aurdino and pump. Methylene blue tests indicated that the flow field was laminar, non-uniform, and stable after < 250 ms of pump onset (data not shown; Supplementary Fig. 3). The flow field had a lateral gradient along the Y-axis that was created by a minute boundary layer of null flow immediately adjacent to the walls and gradually increased (over ~2-5 mm, front to rear) until it became part of the freestream flow field (i.e., blue arrows in Supplementary Fig. 3).

The flume was placed onto a diffused array of 196 LEDs that emitted infrared (IR, 850 nm) light up through a layer of diffusion material (several Kimwipes© sealed in plastic) and the translucent flume (Fig. 1b). A monochromatic high-speed camera (SC1 without IR filter, Edgertronic.com) with a 60 mm manual focus macro lens (Nikon) was placed on a tripod directly over the flume to record behavioral trials at *f*16, 1/1000 s, ISO 20000, and 60 or 200 frames s^{-1} (fps). Videos were saved onto 64 GB SD cards and archived on a 12 TB RAID array (see below) All source files, scripts, details of apparatus construction, and SOP provided online in the Open Source Framework repository, DOI:10.17605/OSF.IO/RVYFZ.).

Lateral Line Isolation and Rheotaxis Trials

To isolate the contribution of the lateral line to rheotaxis, we conducted the behavioral trials under infrared light to eliminate visual cues (Fig. 1a) and reduced linear acceleration cues to the vestibular system by using a flow stimulus that rapidly accelerated (< 250 ms) to a constant maximum velocity (9.74 mm s^{-1}). Angular acceleration was not a factor because larval zebrafish at 6-7dpf cannot detect the angular motion of yaw in the horizontal plane ([31], [32]). Tactile cues were not possible to selectively block in a non-invasive manner.

655 The flume was filled with E3 media (28°C) and the arena placed within the flume. A
656 thermometer was placed into the open portion of the flume to monitor heat generated by the IR
657 lights and miniature ice packs (2 x 2 cm; -20°C) were used to maintain a consistent temperature
658 range of 27-29°C. Under IR illumination, a single larval zebrafish was transferred by pipette from
659 the 6-well plate to the arena within the flume. The swimming activity of the fish was monitored
660 for ~10 s to ensure that it exhibited the burst-and-glide behavior indicative of normal larval
661 zebrafish swimming ([42]). The Arduino was used to begin the trial by using a custom script that
662 triggered the camera to record 10 s of baseline swimming behavior without flow then activate
663 the pump and record 20 s of swimming behavior under flow. After 30 s had elapsed (no flow =
664 0-10 s; initial flow = 10-20 s; and final flow = 20-30 s), the pump and camera turned off and the
665 larvae was removed from the arena. Cohorts of five individual fish from each group (control,
666 neomycin, or $CuSO_4$) were tested before switching to a new group of fish. This process was
667 repeated for up to four iterations during each experimental session (n = 15-20 fish per treatment
668 per session) for a total of 18 sessions (control, n = 248; $CuSO_4$, n = 204; neomycin, n = 222).
669
670 *3D Markerless Pose Estimation (DeepLabCut)*
671 *Equipment:* Our behavioral data acquisition and analysis computer ran on the Windows
672 10 operating system and was based on a Dell Precision 3630 workstation with an Intel Xeon E-
673 2246G processor, 64 GB RAM, multiple 2TB SSD hard drives, EVGA GFORCE RTX 2080Ti
674 video card (GPU), dual 24" 4K monitors, Dell Thunderbolt 3 PCIe Card, OWC Mercury Elite Pro
675 Dock (TB3RSDK24T) - 24TB Thunderbolt 3 Dock and Dual-Drive RAID configured as 12TB
676 RAID 1.
677 *Installation:* Our GPU required Tensorflow 1.12 with the NVIDIA CUDA package to be
678 installed prior to multi-animal DeepLabCut2.2b8 (maDLC; [43], [44]), Python 3.6, and necessary
679 dependencies (https://github.com/DeepLabCut/DeepLabCut/blob/master/docs/installation.md).

680 Detailed tutorials for using maDLC with a single animal are available online
681 (https://github.com/DeepLabCut/DeepLabCut/blob/master/docs/maDLC_AdvUserGuide.md);
682 however, the pertinent details of our procedure are as follows.
683 *Dataset Curation:* To reduce computational load, all video files were downsampled to
684 1000 x 1000 px, dead pixels (i.e., black spots) and extraneous portions of the video were
685 cropped out using the video editor function.
686 *Project Creation:* A single animal maDLC project was created and the project
687 config.yaml file was modified to create and draw a skeleton interconnecting seven unique body
688 parts (left and right eyes, swim bladder, four points along the tail; Fig. 1a) on each larva. A
689 curated set of ten videos provided representative examples of target positive rheotaxis
690 behaviors across experimental treatments, 20 frames were extracted from each video, and the
691 seven body parts labeled on each frame. The annotated frames were checked for accuracy and
692 multiple additional skeletal connections between the seven body parts were added to increase
693 maDLC learning speed and model accuracy.
694 *Pose Estimation:* The training dataset used cropped images (400 x 400 px) to reduce
695 computational loading, Resnet-50 pre-trained network weights, and imgaug data augmentation.
696 We trained the network until all the loss parameters plateaued at 100,000 iterations then it was
697 evaluated (PCK values close to 1, RMSE values low) and cross-validated using the default
698 parameters.
699 *Identity Tracking:* The curated videos were analyzed, and the detections assembled into
700 tracklets using the box method because it provided the best results for our test subjects. The
701 original videos were overlaid with the newly labeled body parts to correct outliers and
702 misidentification of body parts in the tracklet data files.
703 *Post Processing:* The results were plotted for each video and a new labeled video was
704 created to double check for labeling accuracy and ensure there was no need to augment the

705 data set with additional labeled frames. Novel videos were batch processed and analyzed up
706 through the plot trajectories and label videos step.

707

708 *Supervised Behavioral Annotation, Classification, & Analysis (SimBA)*

709 *Definition of Rheotaxis Behavior:* We created a custom Python feature extraction script
710 (file online) that defined positive rheotaxis as when the larvae swam into the oncoming water
711 flow at an angle of 0° ± 45° for at least 100 ms (Supplemental Fig. 1). The tail movement and
712 forward body translation components were used to distinguish active swimming behavior into
713 the flow from passive backward drift with a body angle of 0° ± 45°.

714 *Installation:* SimBAxTF-development version 68 ([45]), Python 3.6, Git, FFmpeg, and all
715 dependencies. (https://github.com/sgoldenlab/simba/blob/master/docs/installation.md).

716 *Dataset Curation*: The pre-processed video files used for maDLC analysis were
717 converted to AVI format using the SimBA video editor function.

718 *Project Creation:* A new SimBA project was created according to the Scenario 1 tutorial:
719 (https://github.com/sgoldenlab/simba/blob/master/docs/Scenario1.md). The user defined pose
720 configuration and DLC-multi animal options were selected prior to generating the project config
721 file. The user-defined pose configuration nomenclature was modified to match the body part and
722 individual animal labels used in the maDLC config.yaml file. A curated set of ten representative
723 rheotaxis behavior videos from each treatment group, along with their associated final tracklet
724 data files created by maDLC, were imported and their frames extracted.

725 *Load Project:* The project was loaded and the video parameters (frame rate (fps),
726 resolution, and pixel measurements (px/mm)) set for each curated video. Outlier correction was
727 achieved using the swim bladder and tail-3 body parts, movement criterion set to 0.7, and
728 location criterion set to 1.5 ([45]). Features were extracted using the custom Python feature
729 extraction script file. Rheotaxis behavior was labeled (i.e., annotations were created for

730 predictive classifiers) for each curated video, save one that was set aside for validation. The
731 default training, hyperparameters, and evaluation settings were used to create the model ([45]).
732 Throughout the earmarked video, the interactive plot function was used to validate the model by
733 determining the probability threshold for the accurate prediction and minimum duration of a
734 rheotaxis event. These values became the discrimination threshold (0.5) and minimum behavior
735 bout length (100 ms) settings used to run the machine model. Naïve videos were processed,
736 behaviors annotated, and machine results data files archived for analysis.
737
738 *Data Analysis*
739 Rheotaxis only occurred when fish swam at angles 0° ± 45° under flow conditions;
740 therefore, the rheotaxis data were compared to data when fish randomly swam at 0° ± 45°
741 under no flow. However, the entire 0-360° body angle datasets were used to determine if the
742 fish from each treatment group were randomly distributed under no flow (Fig. 3), and to
743 determine the X-Y (2D) spatial use under no flow (Fig. 6a) and flow (Fig. 6b) conditions. Time
744 series of rheotaxis data sampled at 200 and 60 Hz (fps) were quantized into their lowest
745 common bin size of 100 ms.
746 Data wrangling and cleaning was performed in R ([46]) with the packages *tidyverse* ([47]),
747 *dplyr* ([48]), *plyr* ([49]), and *readbulk* ([50]). Figures and graphs were created with packages *circular*
748 ([51]), *ggplot2* ([52]), and *viridis* ([53]). The Rayleigh statistical tests (V-test) of uniformity for circular
749 data in a specified mean direction (mu = 0°) and the Watson-Wheeler tests for differences in the
750 grand mean body angle or angular variance (the test does not specify which parameter differs)
751 were performed with the package *CircMLE* ([54]). The mean duration, number, total distance
752 travelled and mean latency to the onset of rheotaxis events were calculated for 10 s bins (i.e.,
753 none, initial, and final flow) using SimBA. These data were analyzed in R using the generalized
754 linear mixed models (GLMM) and post hoc t-tests (Satterthwaite method) in the packages
755 *lmerTest* ([55]) and *lme4* ([56]). The significance values for fixed effects of these GLMM tests are not

reported by those packages and were run separately using the package *stats* ([46]) for type III ANOVAs. The package *zoo* ([57]) was used to convert rheotaxis data into times series and the package *spectral* ([58]) was used to perform the spectral decomposition analysis.

Declaration of interests:

The authors declare no competing financial or non-financial interests.

Acknowledgments: We want to thank Valentin Militchin for the design and construction of the electronic components of the experimental apparatus, David Lee for editorial support, and Mark Warchol for feedback on the manuscript. This work was supported by the National Institute on Deafness and Other Communication Disorders R01DC016066 (L.S.), NIDA R00DA045662 (S.A.G.), NIDA P30 DA048736 (S.R.O.N. and S.A.G.), NARSAD Young Investigator Award 27082 (S.A.G.).

Data Availability

The datasets generated and analyzed during the current study are available in the Open Science Framework repository, DOI 10.17605/OSF.IO/RVYFZ.

Code Availability

The R code generated for the analyses during the current study are available in the Open Science Framework repository, DOI 10.17605/OSF.IO/RVYFZ.

REFERENCES

1 Chagnaud, B. P. & Coombs, S. in *The Lateral Line System* (eds Sheryl Coombs, Horst Bleckmann, Richard R. Fay, & Arthur N. Popper) 151-194 (Springer New York, 2014).

2 Van Trump, W. J. & McHenry, M. J. The lateral line system is not necessary for rheotaxis in the Mexican blind cavefish (Astyanax fasciatus). *Integr Comp Biol* **53**, 799-809, doi:10.1093/icb/ict064 (2013).

3 Lyon, E. P. ON RHEOTROPISM. I. — RHEOTROPISM IN FISHES. *American Journal of Physiology-Legacy Content* **12**, 149-161, doi:10.1152/ajplegacy.1904.12.2.149 (1904).

4 ARNOLD, G. P. RHEOTROPISM IN FISHES. *Biological Reviews* **49**, 515-576, doi:https://doi.org/10.1111/j.1469-185X.1974.tb01173.x (1974).

5 Suli, A., Watson, G. M., Rubel, E. W. & Raible, D. W. Rheotaxis in larval zebrafish is mediated by lateral line mechanosensory hair cells. *PLoS One* **7**, e29727, doi:10.1371/journal.pone.0029727 (2012).

6 Pavlov, D. & Tyuryukov, S. The role of lateral-line organs and equilibrium in the behavior and orientation of the dace, Leuciscus leuciscus, in a turbulent flow. *JOURNAL OF ICHTHYOLOGY C/C OF VOPROSY IKHTIOLOGII* **33**, 45-45 (1993).

7 Pavlov, D. S. & Tjurjukov, S. N. Reactions of dace to linear accelerations. *Journal of Fish Biology* **46**, 768-774, doi:https://doi.org/10.1111/j.1095-8649.1995.tb01600.x (1995).

8 John C. Montgomery, C. F. B. A. G. C. The lateral line can mediate rheotaxis in fish. *Nature*, 960-963 (1997).

9 Baker, C. F. & Montgomery, J. C. Lateral line mediated rheotaxis in the Antarctic fish Pagothenia borchgrevinki. *Polar Biology* **21**, 305-309, doi:10.1007/s003000050366 (1999).

10 Baker, C. F. & Montgomery, J. C. The sensory basis of rheotaxis in the blind Mexican cave fish, Astyanax fasciatus. *Journal of Comparative Physiology A* **184**, 519-527, doi:10.1007/s003590050351 (1999).

11 Dykgraaf, S. Untersuchungen über die Funktion der Seitenorgane an Fischen. *Zeitschrift für vergleichende Physiologie* **20**, 162-214, doi:10.1007/BF00340757 (1933).

12 Bak-Coleman, J., Court, A., Paley, D. A. & Coombs, S. The spatiotemporal dynamics of rheotactic behavior depends on flow speed and available sensory information. *J Exp Biol* **216**, 4011-4024, doi:10.1242/jeb.090480 (2013).

13 Coombs, S., Bak-Coleman, J. & Montgomery, J. Rheotaxis revisited: a multi-behavioral and multisensory perspective on how fish orient to flow. *J Exp Biol* **223**, doi:10.1242/jeb.223008 (2020).

14 Coffin, A. B., Brignull, H., Raible, D. W. & Rubel, E. W. in *The Lateral Line System* (eds Sheryl Coombs, Horst Bleckmann, Richard R. Fay, & Arthur N. Popper) 313-347 (Springer New York, 2014).

15 Harris, J. A. *et al.* Neomycin-Induced Hair Cell Death and Rapid Regeneration in the Lateral Line of Zebrafish (Danio rerio). *Journal of the Association for Research in Otolaryngology* **4**, 219-234, doi:10.1007/s10162-002-3022-x (2003).

16 Ma, E. Y., Rubel, E. W. & Raible, D. W. Notch Signaling Regulates the Extent of Hair Cell Regeneration in the Zebrafish Lateral Line. *The Journal of Neuroscience* **28**, 2261-2273, doi:10.1523/jneurosci.4372-07.2008 (2008).

17 Hardy, K. *et al.* Functional development and regeneration of hair cells in the zebrafish lateral line. *J Physiol* **599**, 3913-3936, doi:10.1113/JP281522 (2021).

18 Kniss, J. S., Jiang, L. & Piotrowski, T. Insights into sensory hair cell regeneration from the zebrafish lateral line. *Current Opinion in Genetics & Development* **40**, 32-40, doi:https://doi.org/10.1016/j.gde.2016.05.012 (2016).

19 Pickett, S. B. & Raible, D. W. Water Waves to Sound Waves: Using Zebrafish to Explore Hair Cell Biology. *J Assoc Res Otolaryngol* **20**, 1-19, doi:10.1007/s10162-018-00711-1 (2019).
20 Olive, R. *et al.* Rheotaxis of Larval Zebrafish: Behavioral Study of a Multi-Sensory Process. *Front Syst Neurosci* **10**, 14, doi:10.3389/fnsys.2016.00014 (2016).
21 Olszewski, J., Haehnel, M., Taguchi, M. & Liao, J. C. Zebrafish larvae exhibit rheotaxis and can escape a continuous suction source using their lateral line. *PLoS One* **7**, e36661, doi:10.1371/journal.pone.0036661 (2012).
22 Oteiza, P., Odstrcil, I., Lauder, G., Portugues, R. & Engert, F. A novel mechanism for mechanosensory-based rheotaxis in larval zebrafish. *Nature* **547**, 445-448, doi:10.1038/nature23014 (2017).
23 Hernández, P. P., Moreno, V., Olivari, F. A. & Allende, M. L. Sub-lethal concentrations of waterborne copper are toxic to lateral line neuromasts in zebrafish (Danio rerio). *Hearing Research* **213**, 1-10, doi:https://doi.org/10.1016/j.heares.2005.10.015 (2006).
24 Linbo, T. L., Stehr, C. M., Incardona, J. P. & Scholz, N. L. Dissolved copper triggers cell death in the peripheral mechanosensory system of larval fish. *Environmental Toxicology and Chemistry* **25**, 597-603, doi:https://doi.org/10.1897/05-241R.1 (2006).
25 Olivari, F. A., Hernández, P. P. & Allende, M. L. Acute copper exposure induces oxidative stress and cell death in lateral line hair cells of zebrafish larvae. *Brain Research* **1244**, 1-12, doi:https://doi.org/10.1016/j.brainres.2008.09.050 (2008).
26 Williams, J. A. & Holder, N. Cell turnover in neuromasts of zebrafish larvae. *Hearing Research* **143**, 171-181, doi:https://doi.org/10.1016/S0378-5955(00)00039-3 (2000).
27 Coffin, A. B., Rubel, E. W. & Raible, D. W. Bax, Bcl2, and p53 differentially regulate neomycin- and gentamicin-induced hair cell death in the zebrafish lateral line. *J Assoc Res Otolaryngol* **14**, 645-659, doi:10.1007/s10162-013-0404-1 (2013).
28 Buck, L. M., Winter, M. J., Redfern, W. S. & Whitfield, T. T. Ototoxin-induced cellular damage in neuromasts disrupts lateral line function in larval zebrafish. *Hear Res* **284**, 67-81, doi:10.1016/j.heares.2011.12.001 (2012).
29 Bak-Coleman, J. & Coombs, S. Sedentary behavior as a factor in determining lateral line contributions to rheotaxis. *J Exp Biol* **217**, 2338-2347, doi:10.1242/jeb.102574 (2014).
30 Elder, J. & Coombs, S. The influence of turbulence on the sensory basis of rheotaxis. *J Comp Physiol A Neuroethol Sens Neural Behav Physiol* **201**, 667-680, doi:10.1007/s00359-015-1014-7 (2015).
31 Beck, J. C., Gilland, E., Tank, D. W. & Baker, R. Quantifying the Ontogeny of Optokinetic and Vestibuloocular Behaviors in Zebrafish, Medaka, and Goldfish. *Journal of Neurophysiology* **92**, 3546-3561, doi:10.1152/jn.00311.2004 (2004).
32 Mo, W., Chen, F., Nechiporuk, A. & Nicolson, T. Quantification of vestibular-induced eye movements in zebrafish larvae. *BMC Neurosci* **11**, 110, doi:10.1186/1471-2202-11-110 (2010).
33 Liao, J. C. The role of the lateral line and vision on body kinematics and hydrodynamic preference of rainbow trout in turbulent flow. *J Exp Biol* **209**, 4077-4090, doi:10.1242/jeb.02487 (2006).
34 Hernandez, P. P. *et al.* Sublethal concentrations of waterborne copper induce cellular stress and cell death in zebrafish embryos and larvae. *Biological Research* **44**, 7-15 (2011).
35 Toro, C. *et al.* Dopamine Modulates the Activity of Sensory Hair Cells. *J Neurosci* **35**, 16494-16503, doi:10.1523/JNEUROSCI.1691-15.2015 (2015).
36 Zhang, Q. *et al.* Synaptically silent sensory hair cells in zebrafish are recruited after damage. *Nat Commun* **9**, 1388, doi:10.1038/s41467-018-03806-8 (2018).

37 Johansen, J. L., Fulton, C. J. & Bellwood, D. R. Avoiding the flow: refuges expand the swimming potential of coral reef fishes. *Coral Reefs* **26**, 577-583, doi:10.1007/s00338-007-0217-y (2007).

38 Webb, P. W. Entrainment by river chub nocomis micropogon and smallmouth bass micropterus dolomieu on cylinders. *J Exp Biol* **201 (Pt 16)**, 2403-2412 (1998).

39 Burt de Perera, T. B. & Braithwaite, V. A. Laterality in a non-visual sensory modality--the lateral line of fish. *Curr Biol* **15**, R241-242, doi:10.1016/j.cub.2005.03.035 (2005).

40 Nusslein-Volhard, C. & Dahm, R. *Zebrafish*. (Oxford University Press, 2002).

41 Han, E. et al (2020 Analysis of behavioral changes in zebrafish (Danio rerio) larvae caused by aminoglycoside-induced damage to the lateral line and muscles. *Neurotoxicology* 78, 134-142, doi: 10.1016/j.neuro.2020.03.005

42 Budick, S. A. & O'Malley, D. M. Locomotor repertoire of the larval zebrafish: swimming, turning and prey capture. *Journal of Experimental Biology* **203**, 2565-2579, doi:10.1242/jeb.203.17.2565 (2000).

43 Mathis, A. *et al.* DeepLabCut: markerless pose estimation of user-defined body parts with deep learning. *Nature Neuroscience* **21**, 1281-1289, doi:10.1038/s41593-018-0209-y (2018).

44 Nath, T. *et al.* Using DeepLabCut for 3D markerless pose estimation across species and behaviors. *Nature Protocols* **14**, 2152-2176, doi:10.1038/s41596-019-0176-0 (2019).

45 Nilsson, S. R. O. *et al.*, doi:10.1101/2020.04.19.049452 (2020).

46 R Core Team (2020). R: A language and environment for statistical computing. R Foundation for Statistical Computing, Vienna, Austria. URL https://www.R-project.org/.

47 Wickham et al., (2019). Welcome to the tidyverse. Journal of Open Source Software, 4(43), 1686, https://doi.org/10.21105/joss.01686

48 Wickham, H., François, R., Henry, L, and Müller, K. (2021). dplyr: A Grammar of Data Manipulation. R package version 1.0.3. https://CRAN.R-project.org/package=dplyr

49 Wickham, H. (2011). The Split-Apply-Combine Strategy for Data Analysis. Journal of Statistical Software, 40(1), 1-29. URL http://www.jstatsoft.org/v40/i01/.

50 Kieslich, P. J., and Henninger, F. (2016). Readbulk: An R package for reading and combining multiple data files. https://doi.org/10.5281/zenodo.596649

51 Agostinelli C. and Lund, U. (2017). R package 'circular': Circular Statistics (version 0.4-93). URL https://r-forge.r-project.org/projects/circular/

52 Wickham, H. ggplot2: Elegant Graphics for Data Analysis. Springer-Verlag New York, 2016.

53 Garnier, S. (2018). viridis: Default Color Maps from 'matplotlib'. R package version 0.5.1.https://CRAN.R-project.org/package=viridis

54 Fitak, R. R. and Johnsen, S. (2017). Bringing the analysis of animal orientation data full circle: model-based approaches with maximum likelihood. Journal of Experimental Biology, 220, 3878-3882. doi:10.1242/jeb.167056

55 Kuznetsova A, Brockhoff PB, Christensen RHB (2017). “lmerTest Package: Tests in Linear Mixed Effects Models.” Journal of Statistical Software_, *82*(13), 1-26. doi: 10.18637/jss.v082.i13 (URL:https://doi.org/10.18637/jss.v082.i13).

56 Bates, D., Maechler, M., Bolker, B., Walker, S. (2015). Fitting Linear Mixed-Effects Models Using lme4. Journal of Statistical Software, 67(1), 1-48. doi:10.18637/jss.v067.i01.

57 Zeileis, A. and Grothendieck, G. (2005). zoo: S3 Infrastructure for Regular and Irregular Time Series. Journal of Statistical Software, 14(6), 1-27. doi:10.18637/jss.v014.i06

58 Seilmayer, M. (2021). spectral: Common Methods of Spectral Data Analysis. R package version 2.0. https://CRAN.R-project.org/package=spectral

925 **SUPPLEMENTARY INFORMATION**

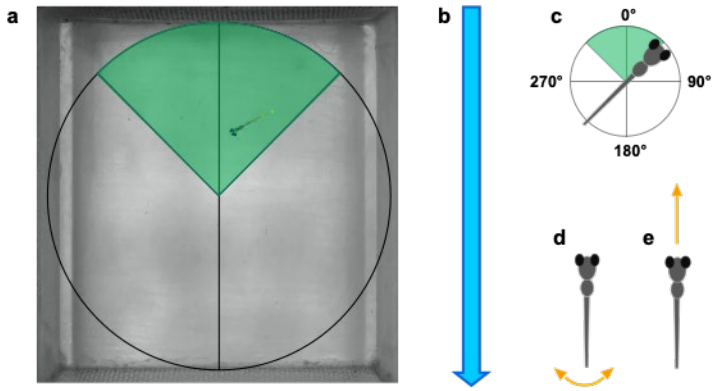

926

927 **Supplementary Figure 1. Definition of positive rheotaxis behavior.** a) Larval zebrafish in the microflume arena performing
928 rheotaxis under flow as defined by multiple conditions, including b) the water flow stimulus was on; c) the fish body angle was
929 oriented to 0° ± 45° (green shaded wedge); d) the tail moved laterally every 100 ms; and e) the body of the fish had forward
930 translation every 100 ms. Note that conditions (d) and (e) were used to discriminate between fish displaying positive rheotaxis and
931 those passively drifting backward with body angles of 0° ± 45°.

932

933

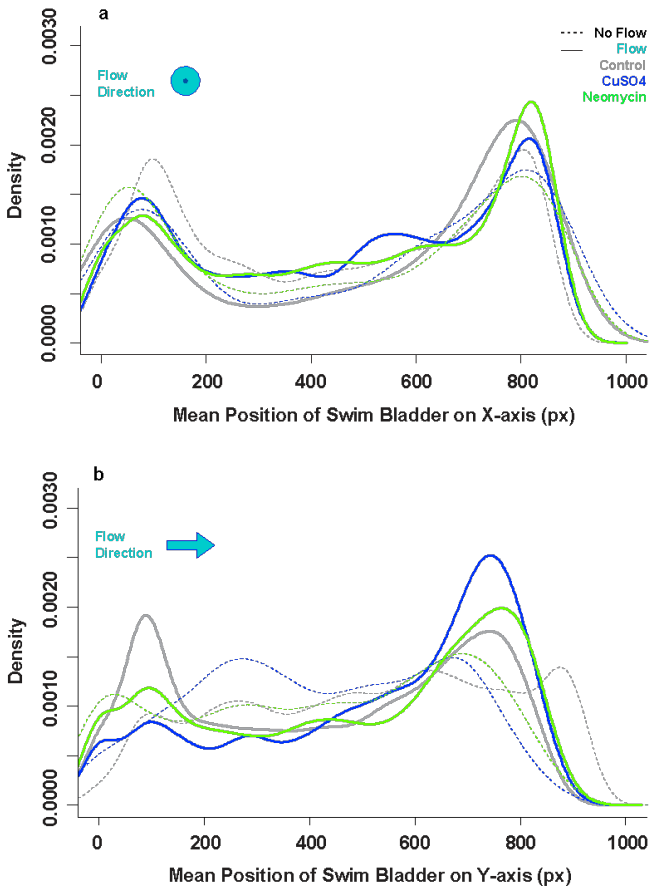

934

935 **Supplemental Figure 2. Intact lateral line allowed fish to hold their position near the source of the flow.** a) The total spatial
936 use of the arena in the X- dimension (left to right) does not differ among treatments (gray = control, blue = $CuSO_4$, green =
937 neomycin) or flow conditions (none = dotted lines, flow = solid lines). All fish preferred to occupy the right versus the left side of the
938 arena. b) in the Y- dimension (front to back) under no flow conditions, the $CuSO_4$ treated fish occupied the center of the arena more
939 than the control or neomycin treated fish. However, under flow conditions, the lateral line intact (control; gray solid line) fish occupied
940 the front of the arena, whereas lesioned fish (blue and green solids lines) predominantly occupied the back of the arena.

941

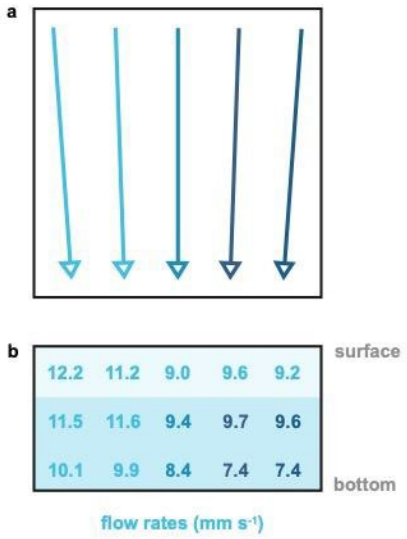

Supplementary Figure 3. Visualization of methylene blue dye tests within the experimental arena shows a laminar yet non-uniform flow field. a) The vectors are color coded according to the mean of the b) cross-sectional flow values (mm s^{-1}) from top to bottom. Each cross-sectional flow value (b) is the mean of five trials. Fish typically occupied the dark shaded area in the bottom two-thirds of the water column and very rarely swam near the surface.

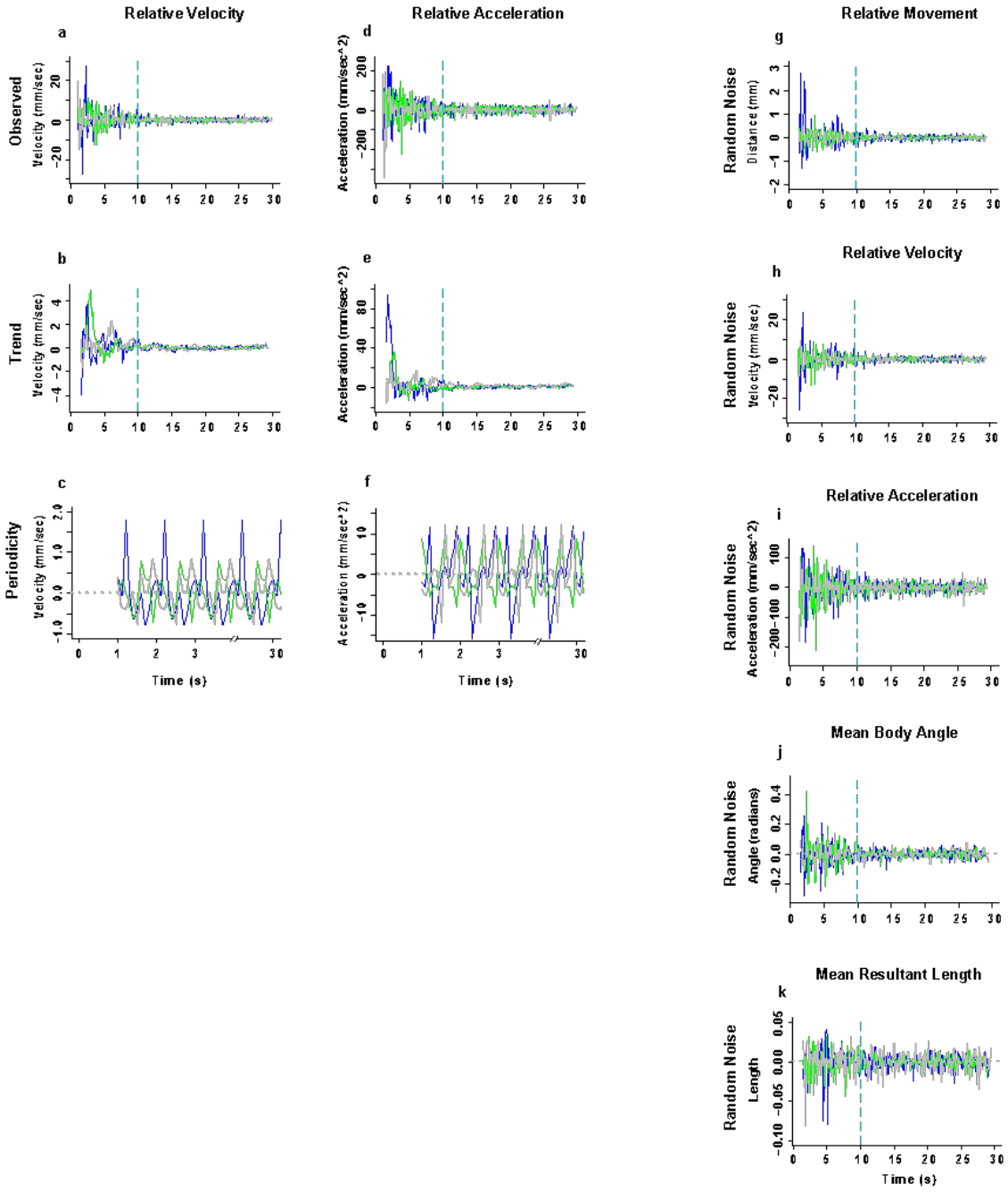

Supplementary Figure 4. The overall trends and periodic fluctuations in the relative velocity and acceleration in rheotaxis behavior differed among treatment groups. Gray = control (n = 248), blue = $CuSO_4$ (n = 204), green = neomycin (n =222). Spectral decomposition of the observed data (a, d) removed the noise (h, i) to reveal the overall underlying trends (b, e) and the periodicity, or recurring fluctuations (c, f) that occurred during any given 1 s of the experiment. The periodicity waveform peaks indicate the average amount (amplitude), number, direction (positive = increasing; negative = decreasing), and order of occurrence for these cyclic fluctuations as a function of unit time (1 s). The overall trends were that there were no differences in relative (b) velocity or (e) acceleration among groups. The periodic fluctuation in relative velocity (c) and acceleration (f) was greatest in $CuSO_4$ treated fish compared to control or neomycin treated fish. The noise for relative movement (g), mean body angle (j), and mean resultant length (k) are shown.

958

	No Flow Stimulus 1-10s *theta, rho,* ang var	Flow Stimulus 11-20s *theta, rho,* ang var	Flow Stimulus 21-30s *theta, rho,* ang var
Control	135.5° 0.084 0.916	357.9° 0.687 0.313	1.7° 0.688 0.312
CuSO4	84.8 ° 0.099 0.901	10.8° 0.530 0.470	3.1° 0.611 0.389
Neomycin	86.7° 0.090 0.900	6.1° 0.656 0.344	6.7° 0.655 0.345

959
960 **Supplementary Table 1.** Grand mean body angle vector parameters. *Theta* = group mean body angle; *rho* = mean length of
961 resultant vector, where 0 = uniform distribution of individual mean body angles, 1 = perfect alignment individual mean body angles;
962 angular variance = 1-*rho*.
963
964
965

	No Flow Stimulus 1-10s test stat, p-value	Flow Stimulus 11-20s test stat, p-value	Flow Stimulus 21-30s test stat, p-value
Control	-0.0595 0.9079	0.686 **< 0.001**	0.6678 **< 0.001**
CuSO4	0.009 0.4276	0.5204 **< 0.001**	0.6105 **< 0.001**
Neomycin	0.0052 0.4566	0.6522 **< 0.001**	0.6507 **< 0.001**

966
967 **Supplementary Table 2.** Rayleigh test of uniformity (V-test) for an expected grand mean body angle, *mu* = 0°. Among all
968 treatments, groups under no flow were not significantly aligned to 0°, whereas groups under flow conditions were significantly
969 aligned to 0°.
970
971

	CTL-10s p-value	CTL-20s p-value	Cu-10s p-value	Cu-20s p-value	Neo-10s p-value	Neo-20s p-value
CTL-10s test stat	-	0.4747	**2.58e-05**	0.119	**0.0357**	>0.10
CTL-20s test stat	1.49	-	**7.041e-05**	**0.0508**	0.07419	0.4502
Cu-10s test stat	21.128	19.122	-	0.04975	0.05861	**0.0090**
Cu-20s test stat	4.2573	5.9597	6.0014	-	0.311	0.1921
Neo-10s test stat	6.6655	5.2022	5.6737	2.3357	-	0.7364
Neo-20s test stat	0.1251	1.5961	9.4268	3.3000	0.61196	-

Supplementary Table 3. Watson Wheeler test for differences in either grand mean body angle or the distribution of the individual mean angles (*the test does not specify*) among treatment groups under flow conditions.

977

GLMM	Estimate	Std. Error	df	t value	Pr(>|t|)
Stimulus (No flow v Flow 10s)	1.14950	0.10746	1390	10.697	**< 2e-16 *****
Stimulus (No flow v Flow 20s)	1.62296	0.10746	1390	15.102	**< 2e-16 *****
Treatment (Control v $CuSO_4$)	0.05485	0.11893	2068	0.461	0.64473
Treatment (Control v Neomycin)	0.04574	0.11507	2068	0.398	0.69103
Stim*Treat (CTL-10s v $CuSO_4$-10s)	-0.34246	0.16277	1390	-2.104	**0.03556 ***
Stim*Treat (CTL-20s v $CuSO_4$-20s)	-0.45260	0.16277	1390	-2.781	**0.00550 ****
Stim*Treat (CTL-10s v Neo-10s)	-0.29562	0.15749	1390	-1.877	**0.06072 .**
Stim*Treat (CTL-20s v Neo-20s)	-0.36519	0.15749	1390	-2.319	**0.02055 ***

978

ANOVA (III)	Sum Sq	Mean Sq	NumDF	DenDF	F value	Pr(>F)
Stimulus	660.88	330.44	2	1390	216.7689	**< 2.2e-16 *****
Treatment	29.83	14.92	2	695	9.7842	**6.449e-05 *****
Stim*Treat	15.40	3.85	4	1390	2.5249	**0.03926 ***

979
980 **Supplementary Table 4**. Generalized Linear Mixed Model with Satterthwaite's method of testing for differences among treatments
981 in the mean duration of rheotaxis events. Type III ANOVA yielded significance values for fixed effects and interactions because the
982 LME4 package in R does not identify them in its output. Significance codes: '***' 0.001, '**' 0.01, '*' 0.05, '.' 0.1
983

984

GLMM	Estimate	Std. Error	df	t value	Pr(>|t|)
Stimulus (No flow v Flow 10s)	2.65530	0.15538	1390	17.089	**< 2e-16 *****
Stimulus (No flow v Flow 20s)	2.91667	0.15538	1390	18.771	**< 2e-16 *****
Treatment (Control v $CuSO_4$)	-0.52696	0.21170	1614	-2.489	**0.0129 ***
Treatment (Control v Neomycin)	0.46123	0.20484	1614	2.252	**0.0245 ***
Stim*Treat (CTL-10s v $CuSO_4$-10s)	-0.57687	0.23535	1390	-2.451	**0.0144 ***
Stim*Treat (CTL-20s v $CuSO_4$-20s)	0.05882	0.23535	1390	0.250	0.8027
Stim*Treat (CTL-10s v Neo-10s)	0.09687	0.22772	1390	0.425	0.6706
Stim*Treat (CTL-20s v Neo-20s)	0.05290	0.22772	1390	0.232	0.8163

985

ANOVA (III)	Sum Sq	Mean Sq	NumDF	DenDF	F value	Pr(>F)
Stimulus	3488.9	1744.46	2	1390	547.3568	**< 2.2e-16 *****
Treatment	167.1	83.57	2	695	26.2224	**1.049e-11 *****
Stim*Treat	40.0	9.99	4	1390	3.1356	**0.01403 ***

986
987 **Supplementary Table 5**. Generalized Linear Mixed Model with Satterthwaite's method of testing for differences among treatments
988 in the mean number of rheotaxis events. Type III ANOVA yielded significance values for fixed effects and interactions because the
989 LME4 package in R does not identify them in its output. Significance codes: '***' 0.001, '**' 0.01, '*' 0.05, '.' 0.1
990

GLMM	Estimate	Std. Error	df	t value	Pr(>|t|)
Stimulus (No flow v Flow 10s)	0.70177	0.16338	1721	4.295	**1.84e-05** ***
Stimulus (No flow v Flow 20s)	0.65449	0.16338	1721	4.006	**6.44e-05** ***
Treatment (Control v $CuSO_4$)	0.18141	0.11436	695	1.586	0.11313
Treatment (Control v Neomycin)	0.30691	0.11102	706	2.764	**0.00585** **

ANOVA (III)	Sum Sq	Mean Sq	NumDF	DenDF	F value	Pr(>F)
Stimulus	243.652	81.037	2	1565	38.8494	**< 2.2e-16** ***
Treatment	8.117	3.796	2	699	3.8913	**0.02086** *

Supplementary Table 6. Generalized Linear Mixed Model with Satterthwaite's method of testing for differences among treatments in the total distance travelled during rheotaxis events. GLMM model had no interaction between stimulus and treatment. Type III ANOVA yielded significance values for fixed effects because the LME4 package in R does not identify them in its output. Significance codes: '***' 0.001, '**' 0.01, '*' 0.05, '.' 0.1

GLMM	Estimate	Std. Error	df	t value	Pr(>|t|)
Stimulus (No flow v Flow 10s)	8.460e+00	3.333e-01	2.085e+03	25.386	**< 2e-16 *****
Stimulus (No flow v Flow 20s)	1.762e+01	3.333e-01	2.085e+03	52.882	**< 2e-16 *****
Treatment (Control v $CuSO_4$)	-1.384e+00	3.569e-01	2.085e+03	-3.877	**0.000109 *****
Treatment (Control v Neomycin)	8.802e-03	2.085e+03	2.085e+03	0.025	0.979669
Stim*Treat (CTL-10s v $CuSO_4$-10s)	.904e-01	5.048e-01	2.085e+03	0.972	0.331412
Stim*Treat (CTL-20s v $CuSO_4$-20s)	1.015e+00	5.048e-01	2.085e+03	2.011	**0.044503 ***
Stim*Treat (CTL-10s v Neo-10s)	-4.100e-02	4.884e-01	2.085e+03	-0.084	0.933106
Stim*Treat (CTL-20s v Neo-20s)	8.078e-02	4.884e-01	2.085e+03	0.165	0.868645

ANOVA (III)	Sum Sq	Mean Sq	NumDF	DenDF	F value	Pr(>F)
Stimulus	112476	56238	2	2089	3834.664	**< 2.2e-16 *****
Treatment	345	173	2	2089	11.764	**8.306e-06 *****

Supplementary Table 7. Generalized Linear Mixed Model with Satterthwaite's method of testing for differences among treatments in the mean latency to the onset of first rheotaxis event. GLMM model had no interaction between stimulus and treatment. Type III ANOVA yielded significance values for fixed effects and interactions because the LME4 package in R does not identify them in its output. Significance codes: '***' 0.001, '**' 0.01, '*' 0.05, '.' 0.1

GLM	Estimate	Std. Error	t value	Pr(>|t|)
Treatment (Control v $CuSO_4$)	31.9668	4.4820	7.132	**1.21e-12 *****
Treatment (Control v Neomycin)	14.6849	4.0870	3.593	**0.000332 *****
ROI (Back v Center)	4.6943	4.7014	0.998	0.318122
ROI (Back v Front)	-6.3503	4.7014	-1.351	0.176878
ROI (Back v Left)	-13.8344	4.7014	-2.943	**0.003278 ****
ROI (Back v Right)	7.7325	4.7014	-1.645	0.100126
ROI*Treat (CTL-Back v $CuSO_4$-Center)	10.2432	6.3386	1.616	0.106188
ROI*Treat (CTL-Back v Neo-Center)	733.35	5.7799	3.287	**0.001023 ****
ROI*Treat (CTL-Back v $CuSO_4$-Front)	18.9995	6.3386	-4.265	**2.05e-05 *****
ROI*Treat (CTL-Back v Neo-Front)	-27.0351	5.7799	0.146	0.884161
ROI*Treat (CTL-Back v $CuSO_4$-Left)	-23.8271	6.3386	-3.759	**0.000174 *****
ROI*Treat (CTL-Back v Neo-Left)	-13.3969	5.7799	-2.318	**0.020519 ***
ROI*Treat (CTL-Back v $CuSO_4$-Right)	-21.5175	6.3386	-3.395	**0.000695 *****
ROI*Treat (CTL-Back v Neo-Right)	-10.7854	5.7799	-1.866	**0.062127 .**

ANOVA (III)	Sum Sq	Mean Sq	Df	F value	Pr(>F)
Treatment	172565	86283	2	49.727	**< 2.2e-16 *****
ROI	778750	194687	4	112.204	**< 2.2e-16 *****
Treatment*ROI	135133	16892	8	9.735	**1.93e-13 *****

Supplementary Table 8. Generalized Linear Model tests for differences in the two-dimensional X-Y spatial use among treatments. GLM model included fixed effects of stimulus and treatment, and the effect of the interaction between stimulus and treatment. ANOVA yielded significance values for fixed effects and interactions because the LME4 package in R does not identify them in its output. Significance codes: '***' 0.001, '**' 0.01, '*' 0.05, '.' 0.1

	Control	Control	Control	$CuSO_4$	$CuSO_4$	$CuSO_4$	Cu-Ctl	Cu-Ctl	Neomycin	Neomycin	Neomycin	Neo-Ctl	Neo-Ctl
Variable	Min	Max	Range	Min	Max	Range	ΔRange	ΔRange (factor)	Min	Max	Range	ΔRange	ΔRange (factor)
mov	-0.0431	0.0583	0.1014	-0.0724	0.1547	0.2270	0.1257	**2.2400**	-0.0414	0.0441	0.0855	-0.0158	*0.8437*
vel	-0.7762	0.8416	1.6178	-0.7991	1.7910	2.5900	0.9723	**1.6010**	-0.7129	0.7997	1.5126	-0.1051	*0.9350*
acc	-11.8950	12.3300	24.2250	-15.8962	12.1951	28.0914	3.8664	**1.1596**	-8.1738	9.7733	17.9471	-6.2779	*0.7409*
angle	-0.0158	0.0107	0.0265	-0.0087	0.0145	0.0231	-0.0034	*0.8729*	-0.0162	0.0256	0.0418	0.0153	**1.5766**
res L	-0.0052	0.0075	0.0127	-0.0038	0.0023	0.0061	-0.0066	*0.4832*	-0.0026	0.0028	0.0054	-0.0074	*0.4219*

Supplementary Table 9 (Based on Fig. 8c, g, k, o, s). Lateral line ablation by drug treatment (Cu, Neo) shifts the range in overall amplitude of linear (*mov, vel, acc*) and angular (*angle, res L*) seasonality data relative to those of the control (Ctl) group. Movement parameters in which the amplitude increased in treatment fish relative to controls are indicated in **bold**, whereas those that decreased are in *italics*.

		Control	$CuSO_4$	Cu-Ctl	Cu-Ctl	Neomycin	Neo-Ctl	Neo-Ctl	Control	$CuSO_4$	Cu-Ctl	Cu-Ctl	Neomycin	Neo-Ctl	Neo-Ctl
Variable	Dominant Peak	Freq (1/s)	Freq	ΔFreq (1/s)	Net Shift Freq 1-3	Freq	ΔFreq (1/s)	Net Shift Freq 1-3	Power	Power	ΔPower (factor)	Net Shift Pwr 1-3	Power	ΔPower (factor)	Net Shift Pwr 1-3
mov	1st	0.1567	0.1528	*-0.0039*	*down*	0.2118	*0.0551*	*down*	0.0169	0.0448	**2.6475**	**up**	0.0337	**1.9964**	**up**
mov	2nd	0.0267	0.1042	*0.0775*	-	0.0139	*-0.0128*	-	0.0101	0.0326	**3.2379**	-	0.0139	**1.3814**	-
mov	3rd	0.2533	0.0208	*-0.2325*	-	0.1632	*-0.0901*	-	0.0082	0.0287	**3.5016**	-	0.0129	**1.5777**	-
vel	1st	0.2533	0.1563	*-0.0971*	*down*	0.2118	*-0.0415*	*down*	1.8444	3.1181	**1.6906**	**up**	6.9068	**3.7447**	**up**
vel	2nd	1.8444	0.2604	*-1.5840*	-	0.4792	*-1.3652*	-	1.5272	2.5076	**1.6419**	-	1.4930	**0.9776**	-
vel	3rd	0.3100	0.2118	*-0.0982*	-	0.1632	*-0.1468*	-	0.7717	1.9820	**2.5683**	-	1.3884	**1.7991**	-
acc	1st	0.2500	0.2604	*0.0104*	*down*	0.2118	*-0.0382*	*down*	363.7884	502.2213	**1.3805**	**up**	938.4990	**2.5798**	**up**
acc	2nd	0.4800	0.3056	*-0.1744*	-	0.4410	*-0.0390*	-	244.0334	402.0855	**1.6477**	-	393.4430	**1.6123**	-
acc	3rd	0.3100	0.1458	*-0.1642*	-	0.2847	*-0.0253*	-	204.4871	304.1066	**1.4872**	-	346.3958	**1.6940**	-
angle	1st	0.0400	0.0382	**-0.0018**	**up**	0.0174	**-0.0226**	**up**	0.0029	0.0042	**1.4571**	**up**	0.0040	**1.3874**	**up**
angle	2nd	0.0700	0.1528	**0.0828**	-	0.1250	**0.0550**	-	0.0026	0.0014	**0.5371**	-	0.0028	**1.0712**	-
angle	3rd	0.1167	0.2083	**0.0917**	-	0.1944	**0.0778**	-	0.0009	0.0009	**1.0510**	-	0.0014	**1.6840**	-
res L	1st	0.0600	0.0313	*-0.0288*	*down*	0.1319	**0.0719**	**up**	0.0002	0.0002	**1.3167**	**up**	0.0001	*0.4215*	*down*
res L	2nd	0.3433	0.0625	*-0.2808*	-	0.2396	**-0.1038**	-	0.0001	0.0001	**1.7516**	-	0.0000	*0.7071*	-
res L	3rd	0.1667	0.1319	*-0.0347*	-	0.4097	**0.2431**	-	0.0001	0.0001	**1.3909**	-	0.0000	*0.6849*	-

Supplementary Table 10 (based on Fig. 9). The primary, secondary, and tertiary dominant frequencies (*Freq*) of the linear (*mov, vel, acc*) and angular (*angle, res L*) movement power spectra shift up or down (*±ΔFreq*) in each of the drug treatments (Cu, Neo) compared to the control (Ctl) group. The peak power (*Pwr*) for all dominant frequencies increases (+*ΔPwr*) in nearly all cases. Values for the net shift in frequency and power were determined by adding the values of the +/- relative shift (ΔFrequency, ΔPower) of all three dominant frequencies and generalizing the overall shift in frequency and power as "up" or "down". The trend of CuSO4 and neomycin ablation results in net downshifts in the frequency and net upshift in power of relative movement, velocity and acceleration and a net upshift in the frequency and power of the mean body angle. However, CuSO4 ablation results in a net downshift in the frequency and net upshift in power, whereas neomycin results in a net upshift in the frequency and net downshift in power. Movement parameters in which the amplitude increased in treatment fish relative to controls are indicated in **bold**, whereas those that decreased are in *italics*.

		Control	Control	$CuSO_4$	$CuSO_4$	Neomycin	Neomycin
Linear parameter reference	Angular parameter CCF	Lag: (+/-) before, after	Heading: right, left Variance: more, less	Lag: (+/-) before, after	Heading: right, left Variance: more, less	Lag: (+/-) before, after	Heading: right, left Variance: more, less
movement	body angle	before	left	**after**	**left**	*after*	*right*
movement	resultant length	before	less	**before**	**less**	*after*	*less*
velocity	body angle	simultaneous	right	*after*	*right*	**after**	**left**
velocity	resultant length	before	less	*after*	*less*	**before**	**less**
acceleration	body angle	**after**	**left**	*after*	*right*	**after**	**left**
acceleration	resultant length	**before**	**less**	*after*	*less*	**before**	**less**

Supplementary Table 11 (based on Fig. 10). The method, and perhaps mechanism, of lateral line ablation by. $CuSO_4$ and neomycin results in two distinct type of rheotaxis kinematics that are different from control fish. Each method has the opposite effect on the linear and angular movement parameters during rheotaxis and neither matches the phenotype of fish with an intact lateral line. Behavioral phenotypes in which an above average increase in the indicated linear variable was strongly correlated with a leftward heading that will occurr later and a decrease in angular variance that occurred previously are indicated in **bold**. Phenotypes in which an above average increase in the indicated linear variable was strongly correlated with a rightward heading and a decrease in angular variance that will occur later are indicated in *italics*.